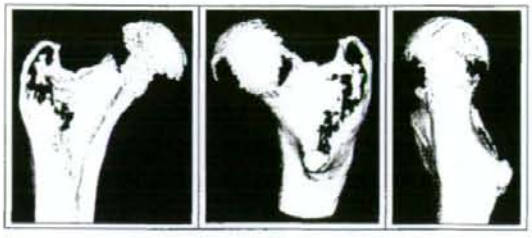

図6
骨粗鬆症女性の大腿骨の三次元CTでは転子間の骨皮質に連続した穿孔像を認める．骨頭下の骨皮質の消失と主応力骨梁の相対的硬化も認められる．

第1とされています．また椎体骨折は「大腿の挙上運動」でも起こります．大腿骨を挙上する大腿筋の起始が第十二胸椎から第二腰椎だからです．すなわち大腿挙上運動の繰り返しで腰椎は強く下方に引かれ椎体骨折も起こります．腰痛体操をやって腰痛が起こるという皮肉な例も多く経験しました．私は転倒防止の筋トレよりも，繰り返しの大腿挙上を控え，「前屈運動」の草取りや「重い物の持ち上げ」などを禁じる注意の方が，よほど有効と思います．

特にまた薬剤治療なしで運動負荷をした場合には骨粗鬆症患者においてはOAの方を進行させて，みかけ上の骨量増加が起こります．大腿骨の立体CTを示します(**図5**)．骨頭下部の吸収が強くなると，中央のprimary median trabeculaで支えることになります．Adams Archとも呼ばれるところですが，皮質骨の吸収消失により負荷の分布が変わりキノコ状，あるいは蛇の頭状に中央部で支えることになってしまいます．中央部の骨梁が過剰に増加しても負荷が加わると外側が折れたり変形してしまいます．

転子部骨折についても，骨折線にあたるところに皮質骨の穿孔が起こります(**図6**)．ビスホスホネートの投与では，本来の皮質骨の回復によって内部のOAにあたる骨梁過剰硬化の減少が起こるのです．ですから，骨折線にあたる部分の骨喪失がはっきり出ている方で，運動を行うということは大腿骨においても骨折の危険が加わるだけでなく，内部のOA硬化が進み，骨量が増えるようにみえるのです．本来はつくべきでない内側について，外部の皮質骨が抜けるという悪循環が観察されるのです．ビスホスホネートの投与では骨粗鬆症から起こる不安定性の改善が最も効果的な治療法になります．

このようなことから，大腿骨頸部骨折予防だけでなくOAの進行防止にも，ビスホスホネート系製剤がベストだと考えます．

岩本　運動の量や質など，まだ検討しなくてはならない点がありますね．

おわりに

岩本　本日は，高齢者の骨粗鬆症について，一般医家の先生方にもわかりやすく，また，明日からの診療にも役立つようなお話をいただきたいということで，それにはどのような検査・治療が必要か，具体的にその場合にどのようなコツや問題点があるかを教えていただきました．

本日はいろいろと有用な情報を提供していただき，ありがとうございました．

文　献

1) Wells GA et al：Alendronate for the primary and secondary prevention of osteoporotic fractures in postmenopausal women. Cochrane Database Syst Rev Jan **23**(1)：CD001155, 2008.
2) Boonen S et al：Safety and efficacy of risedronate in reducing fracture risk in osteoporotic women aged 80 and older：implications for the use of antiresorptive agents in the old and oldest old.

J Am Geriatr Soc **52** : 1832-1839, 2004.
3) Cauley JA et al : Risk of mortality following clinical fracture. Osteoporos Int **11** : 556-561, 2000.
4) Bauer DC et al : Upper Gastrointestinal Tract Safety Profile of Alendronate : The Fracture Intervention Trial. Arch Int Med **160** : 517-525, 2000.
5) Sakamoto K et al : Effects of unipedal standing balance exercise on the prevention of falls and hip fracture among clinically defined high-risk elderly individuals : a randomized controlled trial. J Orthop Sci **11**(5) : 467-472, 2006.

p70 S6 kinase negatively regulates fibroblast growth factor 2-stimulated interleukin-6 synthesis in osteoblasts: function at a point downstream from protein kinase C

S Takai[1], Y Hanai[1,2], R Matsushima-Nishiwaki[1], C Minamitani[1,3], T Otsuka[3], H Tokuda[1,2] and O Kozawa[1]

[1]Department of Pharmacology, Gifu University Graduate School of Medicine, Gifu 501-1194, Japan

[2]Department of Clinical Laboratory, National Center for Geriatrics and Gerontology, National Hospital for Geriatric Medicine, Obu 474-8511, Japan

[3]Department of Orthopedic Surgery, Nagoya City University Graduate School of Medical Sciences, Nagoya 467-8601, Japan

(Correspondence should be addressed to O Kozawa; Email: okozawa@gifu-u.ac.jp)

Abstract

We have previously reported that protein kinase C negatively regulates basic fibroblast growth factor (FGF-2)-stimulated synthesis of interleukin-6 (IL-6), a potent bone resorptive agent, in osteoblast-like MC3T3-E1 cells. To further clarify the mechanism underlying the synthesis of IL-6 in osteoblasts, we investigated whether p70 S6 kinase is involved in the FGF-2-stimulated IL-6 synthesis in these cells. Rapamycin, an inhibitor of p70 S6 kinase, significantly enhanced the FGF-2-stimulated IL-6 synthesis in a dose-dependent manner. Downregulation of p70 S6 kinase by siRNA markedly amplified the FGF-2-stimulated IL-6 synthesis. 12-O-Tetradecanoylphorbol-13-acetate (TPA), a direct activator of protein kinase C, induced the phosphorylation of p70 S6 kinase. Go6976 and bisindolylmaleimide I, inhibitors of protein kinase C, suppressed the TPA-stimulated phosphorylation of p70 S6 kinase. Additionally, protein kinase C inhibitors markedly reduced the phosphorylation of p70 S6 kinase induced by FGF-2. These results strongly suggest that p70 S6 kinase functions at a point downstream of protein kinase C and limits the FGF-2-stimulated IL-6 synthesis in osteoblasts.

Journal of Endocrinology (2008) **197**, 131–137

Introduction

Interleukin-6 (IL-6), which is a multifunctional cytokine that has important physiological effects on a wide range of functions such as promoting B-cell differentiation, T-cell activation, and inducing acute phase proteins (Akira *et al.* 1993, Heymann & Rousselle 2000, Kwan *et al.* 2004), is one of the most potent osteoclastogenic factors (Ishimi *et al.* 1990, Roodman 1992, Akira *et al.* 1993, Kwan *et al.* 2004). Bone metabolism is strictly regulated by two functional cells, osteoblasts and osteoclasts, responsible for bone formation and bone resorption respectively (Nijweide *et al.* 1986). Bone resorption may be enhanced by the increased local production of inflammatory cytokines such as tumor necrosis factor-α and interleukin-1. In osteoblasts (Helle *et al.* 1988, Ishimi *et al.* 1990, Littlewood *et al.* 1991), it has been reported that bone resorptive agents such as tumor necrosis factor-α and interleukin-1 stimulate the synthesis of IL-6. Thus, accumulating evidence indicates that IL-6 secreted from osteoblasts plays a crucial role as a downstream effector of bone resorptive agents.

Osteoblasts synthesize basic fibroblast growth factor (FGF-2), and FGF-2 is embedded in bone matrix (Baylink *et al.* 1993, Hurley *et al.* 1993). It is well known that FGF-2 expression in osteoblasts is detected during fracture repair (Bolander 1992). Therefore, there is no doubt that FGF-2 plays a crucial role in fracture healing, bone remodeling, and osteogenesis (Marie 2003). We have previously reported that FGF-2 autophosphorylates FGF receptors 1 and 2 among four structurally related high-affinity receptors in osteoblast-like MC3T3-E1 cells (Suzuki *et al.* 1996). As for IL-6 synthesis in osteoblasts, we have shown that FGF-2 induces IL-6 synthesis in osteoblasts (Kozawa *et al.* 1997*a*). In addition, we have reported that FGF-2 induces IL-6 synthesis via the activation of p38 MAPK, but also limits the over-synthesis of IL-6 via the activation of protein kinase C pathways (Kozawa *et al.* 1997*a*, 1999). However, the exact mechanism underlying the IL-6 synthesis in osteoblasts remains to be clarified.

It is well recognized that p70 S6 kinase is a mitogen-activated serine/threonine kinase, which is required for cell proliferation and G1 cell cycle progression (Pullen & Thomas 1997). In osteoblasts, it has been shown that fluoroaluminate upregulates p70 S6 kinase phosphorylation (Susa *et al.* 1997). We have previously reported that p70 S6 kinase plays a role as a negative regulator in platelet-derived growth factor BB-stimulated synthesis of IL-6 in osteoblast-like MC3T3-E1 cells (Takai *et al.* 2007*a*). With regard to FGF-2 effect on osteoblasts, we recently demonstrated that FGF-2 induces the activation of p70 S6 kinase in osteoblast-like MC3T3-E1

Journal of Endocrinology (2008) **197**, 131–137
0022-0795/08/0197-131
DOI: 10.1677/JOE-07-0560
Online version via http://www.endocrinology-journals.org

cells, and the activated p70 S6 kinase plays an inhibitory role in the FGF-2-stimulated release of vascular endothelial growth factor (VEGF) through upregulation of stress-activated protein kinase/c-*Jun* N-terminal kinase, composing a negative feedback loop, in osteoblasts (Takai *et al.* 2007*b*). However, the exact role of p70 S6 kinase in osteoblasts has not yet been fully elucidated.

In the present study, we investigated whether p70 S6 kinase is involved in the FGF-2-stimulated IL-6 synthesis in osteoblast-like MC3T3-E1 cells. We here show that p70 S6 kinase activated by FGF-2 negatively regulates IL-6 synthesis at a point downstream from protein kinase C in these cells.

Materials and Methods

Materials

Recombinant human FGF-2 and mouse IL-6 enzyme immunoassay (ELISA) kit was purchased from R&D Systems Inc. (Minneapolis, MN, USA). Rapamycin, bisindolylmaleimide I, Go6976, and calphostin C were obtained from Calbiochem-Novabiochem Co. (La Jolla, CA, USA). 12-*O*-Tetradecanoylphorbol-13-acetate (TPA) was purchased from Sigma Chemical Co. Phospho-specific p70 S6 kinase antibodies were purchased from Cell Signaling Inc. (Beverly, MA, USA). Enhanced chemiluminescence (ECL) Western Blotting Detection System was purchased from Amersham Biosciences. Control short interfering RNA (siRNA; Silencer Negative Control no. 1 siRNA) or p70 S6 kinase siRNA (Silencer Predesigned siRNA, siRNA ID no. 75849, 75755, and 75942) was purchased from Ambion (Austin, TX, USA). siLentFect was purchased from Bio-Rad. Other materials and chemicals were obtained from commercial sources. Rapamycin, TPA, bisindolylmaleimide I, Go6976, and calphostin C were dissolved in dimethyl sulfoxide. The maximum concentration of dimethyl sulfoxide was 0·1%, which did not affect the assay for IL-6 or western blot analysis.

Cell culture

Cloned osteoblast-like MC3T3-E1 cells derived from newborn mouse calvaria (Sudo *et al.* 1993) were maintained as described previously (Kozawa *et al.* 1997*b*). Briefly, the cells were cultured in α-minimum essential medium (α-MEM) containing 10% fetal calf serum (FCS) at 37 °C in a humidified atmosphere of 5% CO_2/95% air. The cells were seeded onto 35 mm (5×10^4) or 90 mm (5×10^5) diameter dishes in α-MEM containing 10% FCS. After 5 days, the medium was exchanged for α-MEM containing 0·3% FCS. The cells were used for experiments after 48 h. Primary cultured osteoblasts were obtained from the calvaria of newborn (1 or 2 days old) balb/c mice as described previously (Yoshida *et al.* 2004). The cells were seeded onto 90 mm diameter dishes (25×10^4 cells) in α-MEM containing 10% FCS. The medium was changed every 3 days until the cells reached confluence. Then, the medium was exchanged for α-MEM containing 0·3% FCS. The cells were used for experiments after 48 h.

IL-6 assay

The cultured cells were stimulated by various doses of FGF-2 in 1 ml α-MEM containing 0·3% FCS for the indicated periods. When indicated, the cells were pretreated with rapamycin for 60 min. The conditioned medium was collected at the end of the incubation, and the IL-6 concentration was measured by ELISA kit according to the manufacturer's instruction. The assay kit can detect the mouse IL-6 in the range between 7·8 and 250 pg/ml. When the samples generate values greater than 250 pg/ml, the samples were adequately diluted with calibrator diluent provided with the kit and re-assayed. The absorbance of ELISA samples was measured at 450 nm with EL 340 Bio Kinetic Reader (Bio-Tek Instruments Inc., Winooski, VT, USA).

Short interfering RNA transfection

To knock down p70 S6 kinase in MC3T3-E1 cells, the cells were transfected with control siRNA (Silencer Negative Control no. 1 siRNA) or p70 S6 kinase siRNA (Silencer Predesigned siRNA, siRNA ID no. 75849, 75755, and 75942, Ambion) using the siLentFect (Bio-Rad) according to the manufacturer's protocol. In brief, the cells were seeded onto 35 mm (1×10^5) diameter dish in α-MEM containing 10% FCS and subcultured for 48 h. After that, the cells were incubated at 37 °C for 48 h with 250 nM siRNA–siLentFect complexes. As a result, we confirmed that siRNA ID no. 75849 had a most prominent effect to silence the p70 S6 kinase among these three siRNAs. The siRNA ID no. 75849 caused ~80% reduction in the p70 S6 kinase levels compared with those of control siRNA (Takai *et al.* 2007*b*). Then, we used siRNA ID no. 75849 in the experiment of the effect of p70 S6 kinase downregulation on the FGF-2 stimulated IL-6 synthesis.

Western blot analysis

The cultured cells were stimulated by TPA or FGF-2 in α-MEM containing 0·3% FCS for the indicated periods. When indicated, the cells were pretreated with bisindolylmaleimide I, Go6976, and calphostin C for 60 min. The cells were washed twice with PBS and then lysed, homogenized, and sonicated in a lysis buffer containing 62·5 mM Tris–HCl (pH 6·8), 2% SDS, 50 mM dithiothreitol, and 10% glycerol. The cytosolic fraction was collected as a supernatant after centrifugation at 125 000 ***g*** for 10 min at 4 °C. SDS-PAGE was performed according to Laemmli (1970) in 10% polyacrylamide gel. Western blot analysis was performed as described previously (Kato *et al.* 1996) using phospho-specific p70 S6 kinase antibodies and p70 S6 kinase antibodies, with peroxidase-labeled antibodies raised in goat against rabbit IgG being used as secondary antibodies. Peroxidase activity on the

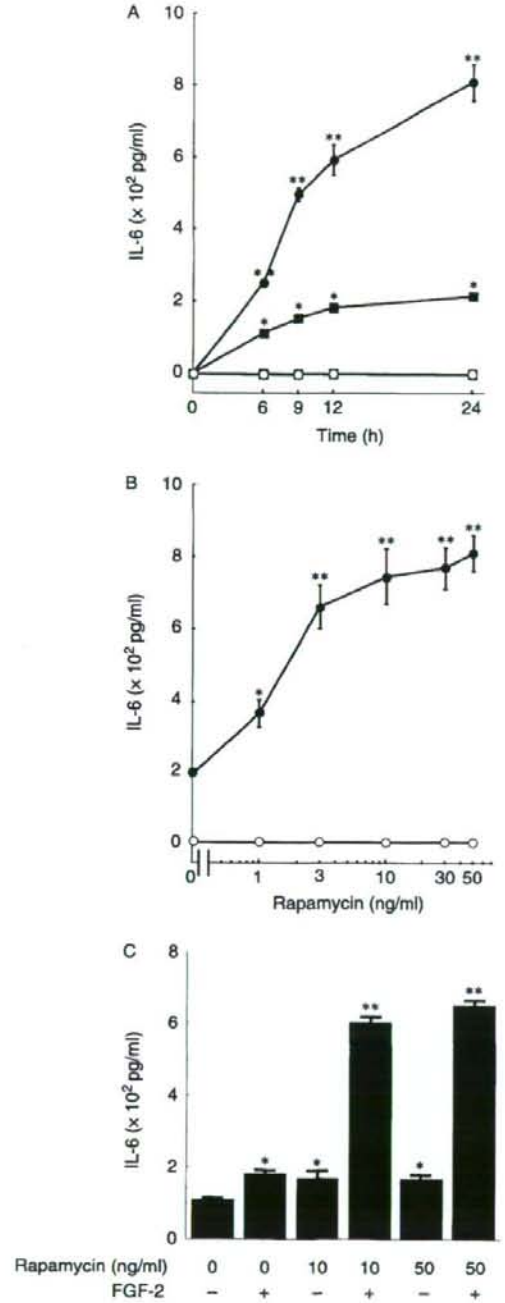

polyvinylidene fluoride (PVDF) sheet was visualized on X-ray film by means of the ECL Western Blotting Detection System. The densitometric analysis was performed using Molecular Analyst/Macintosh (Bio-Rad Laboratories).

Statistical analysis

The data were analyzed by ANOVA followed by the Bonferroni method for multiple comparisons between pairs, and $P<0.05$ was considered significant. All data are presented as the mean + S.E.M. of triplicate determinations from three independent cell preparations. Each experiment was repeated three times with similar results.

Results

Effect of rapamycin on the FGF-2-stimulated IL-6 synthesis in MC3T3-E1 cells

We have previously shown that FGF-2 induces the activation of p70 S6 kinase in osteoblast-like MC3T3-E1 cells (Takai *et al.* 2007*b*). In addition, we have also previously reported that the levels of phosphorylated p70 S6 kinase reached its peak at 45 minutes after the stimulation of FGF-2 and decreased thereafter (Takai *et al.* 2007*b*). In order to clarify the involvement of p70 S6 kinase in the FGF-2-induced synthesis of IL-6 in MC3T3-E1 cells or not, we examined the effect of rapamycin, a specific inhibitor of p70 S6 kinase (Kuo *et al.* 1992, Price *et al.* 1992), on the FGF-2-stimulated synthesis of IL-6. We have previously showed that FGF-2 induces IL-6 synthesis by MC3T3-E1 cells in a time-dependent manner (Kozawa *et al.* 1997*a*). Rapamycin, which had no effect on the basal levels of IL-6, significantly amplified the FGF-2-induced synthesis of IL-6 in a time-dependent manner. The amplifying effect of rapamycin was observed at least 6 h after FGF-2 stimulation (Fig. 1A). In addition, the amplifying effect of rapamycin was dose dependent in the range between 1 and 50 ng/ml (Fig. 1B). Rapamycin at 50 ng/ml caused ~300% enhancement in the FGF-2 effect. We next examined the effect of rapamycin

Figure 1 Effect of rapamycin on the FGF-2-stimulated IL-6 synthesis in osteoblasts. (A) Osteoblast-like MC3T3-E1 cells were pretreated with 10 ng/ml rapamycin (circles) or vehicle (squares) for 60 min, and then stimulated by 70 ng/ml FGF-2 (solid symbols) or vehicle (open symbols) for the indicated periods. *$P<0.0005$, compared with the control. **$P<0.0005$, compared with the value of FGF-2 alone. (B) Osteoblast-like MC3T3-E1 cells were pretreated with various doses of rapamycin for 60 min, and then stimulated by 70 ng/ml FGF-2 (●) or vehicle (○) for 24 h. *$P<0.001$, compared with the value of FGF-2 alone. **$P<0.0005$, compared with the value of FGF-2 alone. (C) Primary culture of osteoblasts was pretreated with various doses of rapamycin for 60 min, and then stimulated by 70 ng/ml FGF-2 or vehicle for 24 h. *$P<0.01$, compared with value of the control. **$P<0.005$, compared with the value of FGF-2 alone. (A–C) Each value represents the mean ± S.E.M. of triplicate determinations from three independent cell preparations. Similar results were obtained with two additional experiments.

in primary cultured mouse osteoblasts. We found that FGF-2 significantly induced IL-6 synthesis also in these osteoblasts. In addition, rapamycin significantly increased the FGF-2-stimulated IL-6 synthesis in the range between 10 and 50 ng/ml (Fig. 1C).

Effect of p70 S6 kinase down regulation on the FGF-2-stimulated IL-6 synthesis in MC3T3-E1 cells

To further confirm the enhancement by rapamycin of IL-6 synthesis, we examined the effect of p70 S6 kinase down-regulation by p70 S6 kinase siRNA on the IL-6 synthesis induced by FGF-2 in osteoblast-like MC3T3-E1 cells. We previously found that p70 S6 kinase siRNA (250 nM) caused ~80% reduction in the p70 S6 kinase levels compared with those of control siRNA (Takai *et al.* 2007*b*). In the p70 S6 kinase downregulated cells, the basal levels of IL-6 were upregulated while the levels of IL-6 were undetectable in the control siRNA-transfected cells (Fig. 2). The FGF-2-induced levels of IL-6 synthesis in p70 S6 kinase down-regulated cells were markedly enhanced compared with those in the control cells. Downregulation of p70 S6 kinase caused approximately ten times enhancement in the FGF-2 effect (Fig. 2).

Effect of TPA on the phosphorylation of p70 S6 kinase in MC3T3-E1 cells

In our previous studies (Suzuki *et al.* 1996, Kozawa *et al.* 1997*a*), we have reported that FGF-2 stimulates the activation of protein kinase C through hydrolysis of phospholipase C-induced phosphoinositide and phospholipase D-induced phosphatidylcholine in osteoblast-like MC3T3-E1 cells, and the protein kinase C activation plays an inhibitory role in the FGF-2-stimulated IL-6 synthesis. In order to investigate whether protein kinase C induces p70 S6 kinase activation in MC3T3-E1 cells, we examined the effect of TPA, a direct activator of protein kinase C (Nishizuka 1991), on the phosphorylation of p70 S6 kinase. The stimulation of TPA time dependently induced the phosphorylation of p70 S6 kinase (Fig. 3). The effect of TPA was observed 10 min after the stimulation of FGF-2 and the maximum effect was at 45 min.

Effects of Go6976 or bisindolylmaleimide I on the TPA-induced phosphorylation of p70 S6 kinase in MC3T3-E1 cells

We examined the effect of Go6976, a potent inhibitor of protein kinase C (Martiny-Baron *et al.* 1993), on the TPA-induced phosphorylation of p70 S6 kinase in MC3T3-E1 cells. Go6976 markedly reduced the phosphorylation of p70 S6 kinase (Fig. 4A). The effect of Go6976 was dose dependent in the range between 0·3 and 3 μM. In addition, bisindolylmaleimide I (30 μM), another inhibitor of protein kinase C (Toullec *et al.* 1991), almost completely suppressed the TPA-induced phosphorylation of p70 S6 kinase (Fig. 4B). The effect of bisindolylmaleimide I was dose dependent in the range between 3 and 30 μM.

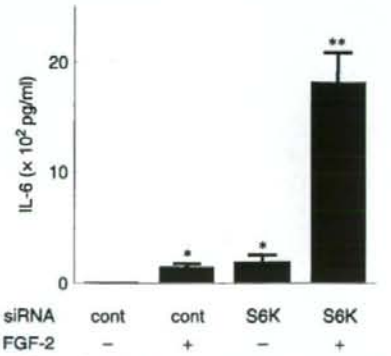

Figure 2 Effect of p70 S6 kinase (S6K) siRNA on the FGF-2-stimulated IL-6 synthesis in MC3T3-E1 cells. The cultured cells were transfected with control siRNA (cont) or p70 S6 kinase siRNA (siRNA ID no. 75849, Ambion; S6K) using the siLentFect according to the manufacturer's protocol. The cells were stimulated by 70 ng/ml FGF-2 or vehicle for 9 h. Each value represents the mean+S.E.M. of triplicate determinations from three independent cell preparations. Similar results were obtained with two additional experiments. *$P<0·0005$, compared with the value of vehicle. **$P<0·0005$, compared with the value of FGF-2 with control siRNA transfection.

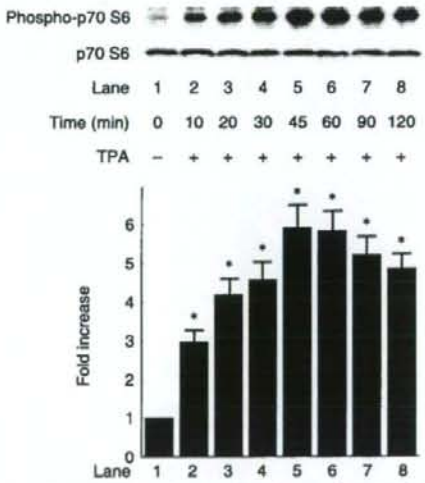

Figure 3 Effect of TPA on the phosphorylation of p70 S6 kinase in MC3T3-E1 cells. The cultured cells were stimulated by 0·1 μM TPA for the indicated periods. The extracts of cells were subjected to SDS–PAGE with subsequent western blot analysis with antibodies against phospho-specific p70 S6 kinase or p70 S6 kinase. The histogram shows quantitative representations of the levels of FGF-2-induced phosphorylation obtained from laser densitometric analysis of three independent experiments. Each value represents the mean±S.E.M. of triplicate determinations from three independent cell preparations. Similar results were obtained with two additional experiments. *$P<0·0001$, compared with the value of control.

Effects of Go6976, bisindolylmaleimide I, or calphostin C on the FGF-2-induced phosphorylation of p70 S6 kinase in MC3T3-E1 cells

We next examined the effects of protein kinase C inhibitors on the FGF-2-induced phosphorylation of p70 S6 kinase in MC3T3-E1 cells. The FGF-2-induced phosphorylation of p70 S6 kinase was markedly attenuated by Go6976 or bisindolylmaleimide I (Fig. 5A and B). Furthermore, calphostin C, an inhibitor of protein kinase C (Kobayashi *et al.* 1989), significantly suppressed the FGF-2-induced phosphorylation of p70 S6 kinase (Fig. 5C). Finally, we confirmed that the suppressive effects of these inhibitors were dose dependent.

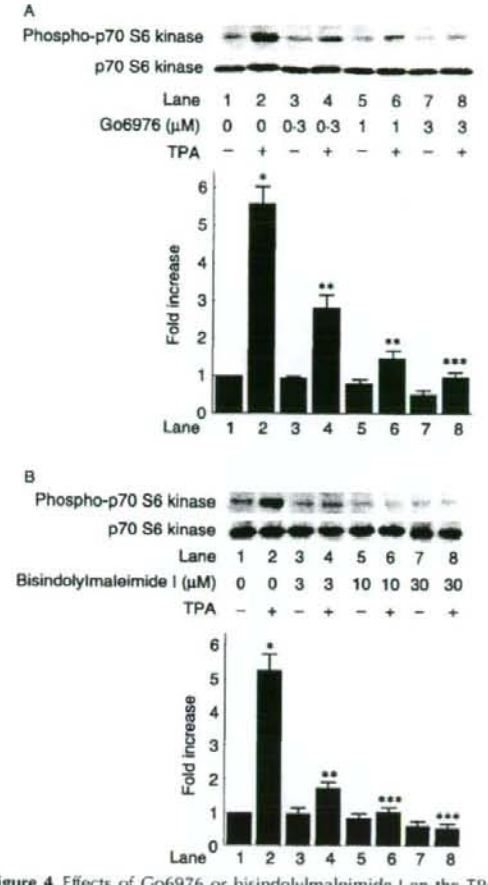

Figure 4 Effects of Go6976 or bisindolylmaleimide I on the TPA-induced phosphorylation of p70 S6 kinase in MC3T3-E1 cells. The cultured cells were pretreated with various doses of Go6976 (A) or 30 μM bisindolylmaleimide I, (B) for 60 min, and then stimulated by 0·1 μM TPA or vehicle for 20 min. The extracts of cells were subjected to SDS–PAGE with subsequent western blot analysis with antibodies against phospho-specific p70 S6 kinase or p70 S6 kinase. (A and B) The histogram shows quantitative representations of the levels of FGF-2-induced phosphorylation obtained from laser densitometric analysis of three independent experiments. Each value represents the mean ± S.E.M. of triplicate determinations from three independent cell preparations. Similar results were obtained with two additional experiments. *P=0·0001, compared with the control. **P<0·005, compared with the value of TPA alone. ***P<0·0005, compared with the value of TPA alone.

Discussion

In our previous study, we showed that FGF-2 stimulated the IL-6 synthesis time dependently up to 48 h, and the effect was dose dependent between 1 and 30 ng/ml (Kozawa *et al.* 1997*a*). In this study, we investigated whether p70 S6 kinase functions in the FGF-2-stimulated IL-6 synthesis or not in these cells. Rapamycin, a specific inhibitor of p70 S6 kinase (Kuo *et al.* 1992, Price *et al.* 1992), significantly amplified the FGF-2-stimulated synthesis of IL-6 in MC3T3-E1 cells. We found that rapamycin enhanced the FGF-2-stimulated IL-6 synthesis also in primary cultured mouse osteoblasts. These findings suggest that suppressive effect by p70 S6K on the FGF-2-stimulated IL-6 synthesis is not specific in a clonal osteoblast-like MC3T3-E1 cells but it is common in osteoblasts. We previously found that rapamycin strongly attenuated the FGF-2-induced phosphorylation of p70 S6 kinase (Takai *et al.* 2007*b*). In addition, the FGF-2-stimulated IL-6 synthesis was enhanced by downregulation of p70 S6 kinase by siRNA in MC3T3-E1. These results strongly suggest that FGF-2-activated p70 S6 kinase suppresses the FGF-2-stimulated IL-6 synthesis. Therefore, it is possible that p70 S6 kinase signaling activated by FGF-2 negatively regulates the FGF-2-induced over-synthesis of IL-6 in osteoblast-like MC3T3-E1 cells.

It is generally recognized that 1) the activity of p70 S6 kinase is regulated by multiple phosphorylation events (Pullen & Thomas 1997) and 2) phosphorylation at Thr389 most strongly correlates with p70 S6 kinase activity among the phosphorylation sites (Pullen & Thomas 1997). In the present study, we demonstrated that TPA time-dependently induced the phosphorylation of p70 S6 kinase at Thr389 in osteoblast-like MC3T3-E1 cells using phospho-specific p70 S6 kinase (Thr389) antibodies. In addition, the TPA-induced phosphorylation of p70 S6 kinase was markedly attenuated by Go6976, a potent inhibitor of protein kinase C. Furthermore, we found that bisindolylmaleimide I, another protein kinase C inhibitor, suppressed the p70 S6 kinase phosphorylation. Based on these results, it is most likely that p70 S6 kinase activation occurs via the activation of protein kinase C in osteoblast-like MC3T3-E1 cells.

We have previously reported that FGF-2 induces the activation of protein kinase C via phosphoinositide hydrolysis and phosphatidylcholine hydrolysis in osteoblast-like MC3T3-E1 cells, resulting in the negative regulation of the FGF-2-stimulated IL-6 synthesis (Suzuki *et al.* 1996, Kozawa *et al.* 1997*a*). Taken together, our findings led us to speculate

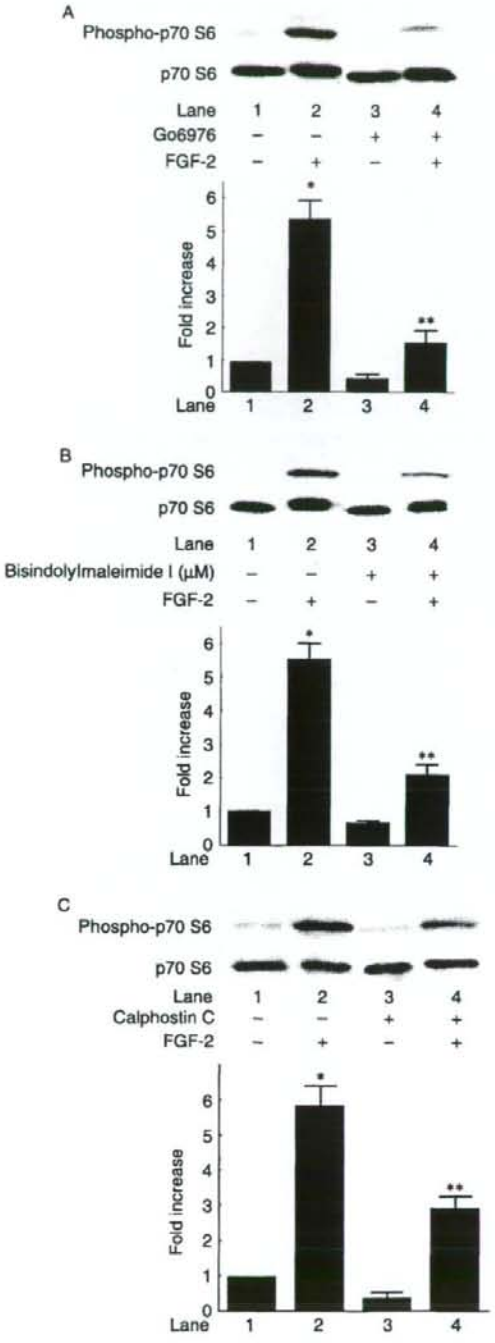

that protein kinase C functions at a point upstream from p70 S6 kinase in the FGF-2-regulated IL-6 synthesis in MC3T3-E1 cells. We showed here that the phosphorylated levels of FGF-2-induced p70 S6 kinase were markedly reduced by Go6976 and bisindolylmaleimide I. In addition, we demonstrated that calphostin C, another type inhibitor of protein kinase C, suppressed the FGF-2-induced phosphorylation of p70 S6 kinase. Taking our findings into account as a whole, it is probable that p70 S6 kinase acts as a negative regulator at a point downstream from protein kinase C in the FGF-2-stimulated IL-6 synthesis in osteoblast-like MC3T3-E1 cells.

It is generally recognized that the p70 S6 kinase pathway plays an important role in various cellular functions, especially cell cycle progression (Pullen & Thomas 1997). Based on our results, it is probable that the p70 S6 kinase pathway in osteoblasts has a pivotal role in the control of the production of IL-6, one of the key factors in bone remodeling. In our previous study (Takai *et al.* 2007*a*), we showed that p70 S6 kinase downregulates platelet-derived growth factor-BB-stimulated IL-6 synthesis in osteoblast-like MC3T3-E1 cells. Since IL-6 is one of the most potent stimulators of osteoclast activity (Kwan *et al.* 2004), our results lead us to speculate that p70 S6 kinase signaling activated by growth factors such as FGF-2 and platelet-derived growth factor-BB in osteoblasts acts as a key regulator to suppress over-synthesizing IL-6, resulting in the prevention of excess bone resorption in the process of bone remodeling. Therefore, the p70 S6 kinase pathway in osteoblasts might be considered to be a new candidate as a molecular target of bone resorption concurrent with various bone diseases. On the other hand, we have recently reported that p70 S6 kinase acts as a negative regulator in the FGF-2-stimulated synthesis of VEGF factor in MC3T3-E1 cells (Takai *et al.* 2007*b*). It is well recognized that VEGF is angiogenic growth factor specific for vascular endothelial cells that provide microvasculature indispensable for bone remodeling (Erlebacher *et al.* 1995, Ferrara & Davis-Smyth 1997). Taking our findings into account as a whole, p70 S6 kinase might play a central role in bone metabolism through the fine-tuning of the local factor network. Further investigation is required to clarify the exact role of p70 S6 kinase in bone metabolism.

Figure 5 Effects of Go6976, bisindolylmaleimide I, or calphostin C on the FGF-2-induced phosphorylation of p70 S6 kinase in MC3T3-E1 cells. The cultured cells were pretreated with 3 μM Go6976 (A), 30 μM bisindolylmaleimide I (B), or 0·7 μM calphostin C (C) for 60 min, and then stimulated by 0·1 μM TPA or vehicle for 20 min. (A–C) The extracts of cells were subjected to SDS–PAGE with subsequent western blot analysis with antibodies against phospho-specific p70 S6 kinase or p70 S6 kinase. The histogram shows quantitative representations of the levels of FGF-2-induced phosphorylation obtained from laser densitometric analysis of three independent experiments. Each value represents the mean ± S.E.M. of triplicate determinations from three independent cell preparations. Similar results were obtained with two additional experiments. *$P = 0{\cdot}0001$, compared with the control. **$P < 0{\cdot}005$, compared with the value of FGF-2 alone.

In conclusion, our results strongly suggest that p70 S6 kinase functions at a point downstream of protein kinase C and limits FGF-2-stimulated IL-6 synthesis in osteoblasts.

Acknowledgements

We are very grateful to Yoko Kawamura and Seiko Sakakibara for their skillful technical assistance. This investigation was supported in part by Grant-in-Aid for Scientific Research (16590873 and 16591482) for the Ministry of Education, Science, Sports and Culture of Japan; the Research Grants for Longevity Sciences (15A-1 and 15C-2); the Research on Proteomics; and the Research on Longevity Sciences from the Ministry of Health, Labour and Welfare of Japan. The authors declare that there is no conflict of interest that would prejudice the impartiality of this scientific work.

References

Akira S, Taga T & Kishimoto T 1993 Interleukin-6 in biology and medicine. *Advances in Immunology* **54** 1–78.

Baylink DJ, Finkleman RD & Mohan S 1993 Growth factor to stimulate bone formation. *Journal of Bone and Mineral Research* **8** S565–S572.

Bolander ME 1992 Regulation of fracture repair by growth factors stimulate tyrosine kinase activity *in vivo*. *Proceedings of the Society for Experimental Biology and Medicine* **200** 165–170.

Erlebacher A, Filvaroff EH, Gitelman SE & Derynck R 1995 Toward a molecular understanding of skeletal development. *Cell* **80** 371–378.

Ferrara N & Davis-Smyth T 1997 The biology of vascular endothelial growth factor. *Endocrine Reviews* **18** 4–25.

Helle M, Brakenhoff JPJ, DeGroot ER & Aarden LA 1988 Interleukin-6 is involved in interleukin-1-induced activities. *European Journal of Immunology* **18** 957–959.

Heymann D & Rousselle AV 2000 gp130 Cytokine family and bone cells. *Cytokine* **12** 1455–1468.

Hurley MM, Abreu C, Harrison JR, Lichtler AC, Raisz LG & Kream BE 1993 Basic fibroblast growth factor inhibits type I collagen gene expression in osteoblastic MC3T3-E1 cells. *Journal of Biological Chemistry* **268** 5588–5593.

Ishimi Y, Miyaura C, Jin CH, Akatsu T, Abe E, Nakamura Y, Yamaguchi Y, Yoshiki S, Matsuda T, Hirano T *et al.* 1990 IL-6 is produced by osteoblasts and induces bone resorption. *Journal of Immunology* **145** 3297–3303.

Kato K, Ito H, Hasegawa K, Inaguma Y, Kozawa O & Asano T 1996 Modulation of the stress-induced synthesis of hsp27 and alpha B-crystallin by cyclic AMP in C6 rat glioma cells. *Journal of Neurochemistry* **66** 946–950.

Kobayashi E, Nakano H, Morimoto M & Tamaoki T 1989 Calphostin C (UCN-1028C), a novel microbial compound, is a highly potent and specific inhibitor of protein kinase C. *Biochemical and Biophysical Research Communications* **159** 548–553.

Kozawa O, Suzuki A & Uematsu T 1997*a* Basic fibroblast growth factor induces interleukin-6 synthesis in osteoblasts: autoregulation by protein kinase C. *Cellular Signalling* **9** 463–468.

Kozawa O, Suzuki A, Tokuda H & Uematsu T 1997*b* Prostaglandin $F_{2\alpha}$ stimulates interleukin-6 via activation of PKC in osteoblast-like cells. *American Journal of Physiology* **272** E208–E211.

Kozawa O, Tokuda H, Matsuno H & Uematsu T 1999 Involvement of p38 mitogen-activated protein kinase in basic fibroblast growth factor-induced interleukin-6 synthesis in osteoblasts. *Journal of Cellular Biochemistry* **74** 479–485.

Kuo CJ, Chung J, Fiorentino DF, Flanagan WM, Blenis J & Crabtree GR 1992 Rapamycin selectively inhibits interleukin-2 activation of p70 S6 kinase. *Nature* **358** 70–73.

Kwan Tat S, Padrines M, Theoleyre S, Heymann D & Fortun Y 2004 IL-6, RANKL, TNF-alpha/IL-1: interrelations in bone resorption pathophysiology. *Cytokine and Growth Factor Reviews* **15** 49–60.

Laemmli LK 1970 Cleavage of structural proteins during the assembly of the head of bacteriophage T4. *Nature* **227** 680–685.

Littlewood AJ, Russil J, Harvey GR, Hughes DE, Russel RGG & Gowen M 1991 The modulation of the expression of IL-6 and its receptor in human osteoblasts *in vitro*. *Endocrinology* **129** 1513–1520.

Marie PJ 2003 Fibroblast growth factor signaling controlling osteoblast differentiation. *Gene* **316** 23–32.

Martiny-Baron G, Kazanietz MG, Mischak H, Blumberg PM, Kochs G, Hug H, Marm D & Schachtele C 1993 Selective inhibition of protein kinase C isozymes by the indolocarbazole Go 6976. *Journal of Biological Chemistry* **268** 9194–9197.

Nijweide PJ, Burger EH & Feyen JHM 1986 Cells of bone: proliferation, differentiation, and hormonal regulation. *Physiological Reviews* **86** 855–886.

Nishizuka Y 1991 Studies and perspectives of protein kinase C. *Science* **233** 305–312.

Price DJ, Grove JR, Calvo V, Avruch J & Bierer BE 1992 Rapamycin-induced inhibition of the 70-kilodalton S6 protein kinase. *Science* **257** 973–977.

Pullen N & Thomas G 1997 The modular phosphorylation and activation of p70s6k. *FEBS Letters* **410** 78–82.

Roodman GD 1992 Interleukin-6: an osteotropic factor? *Journal of Bone and Mineral Research* **7** 475–478.

Sudo H, Kodama H, Amagai Y, Yamamoto S & Kasai S 1993 *In vitro* differentiation and calcification in a new clonal osteogenic cell line derived from newborn mouse calvaria. *Journal of Cell Biology* **96** 191–198.

Susa M, Standke GJ, Jeschke M & Rohner D 1997 Fluoroaluminate induces pertussis toxin-sensitive protein phosphorylation: differences in MC3T3-E1 osteoblastic and NIH3T3 fibroblastic cells. *Biochemical and Biophysical Research Communications* **235** 680–684.

Suzuki A, Shinoda J, Kanda S, Oiso Y & Kozawa O 1996 Basic fibroblast growth factor stimulates phosphatidylcholine-hydrolyzing phospholipase D in osteoblast-like cells. *Journal of Cellular Biochemistry* **63** 491–499.

Takai S, Tokuda H, Hanai Y & Kozawa O 2007*a* Limitation by p70 S6 kinase of PDGF-BB-induced IL-6 synthesis in osteoblast-like MC3T3-E1 cells. *Metabolism* **56** 476–483.

Takai S, Tokuda H, Hanai Y, Harada A, Yasuda E, Matsushima-Nishiwaki R, Kato H, Ogura S, Ohta T & Kozawa O 2007*b* Negative regulation by p70 S6 kinase of FGF-2-stimulated VEGF release through stress-activated protein kinase/c-Jun N-terminal kinase in osteoblasts. *Journal of Bone and Mineral Research* **22** 337–346.

Toullec D, Pianetti P, Coste H, Bellevergue P, Grand-Perret T, Ajakane M, Baudet V, Boissin P, Boursier E, Loriolle F *et al.* 1991 The bisindolylmaleimide GF 109203X is a potent and selective inhibitor of protein kinase C. *Journal of Biological Chemistry* **266** 15771–15781.

Yoshida M, Niwa M, Ishisaki A, Hirade K, Ito H, Shimizu K, Kato K & Kozawa O 2004 Methotrexate enhances prostaglandin D2-stimulated heat shock protein 27 induction in osteoblast. *Prostaglandins, Leukotrienes, and Essential Fatty Acids* **71** 351–362.

Received in final form 4 February 2008
Accepted 5 February 2008
Made available online as an Accepted Preprint
5 February 2008

Life Sciences 82 (2008) 1012-1017

Contents lists available at ScienceDirect

Life Sciences

journal homepage: www.elsevier.com/locate/lifescie

(−)-Epigallocatechin gallate reduces transforming growth factor β-stimulated HSP27 induction through the suppression of stress-activated protein kinase/c-Jun N-terminal kinase in osteoblasts

Kana Hayashi [a], Shinji Takai [a], Rie Matsushima-Nishiwaki [a], Yoshiteru Hanai [a,b], Kanefusa Kato [c], Haruhiko Tokuda [a,b], Osamu Kozawa [a,*]

[a] Department of Pharmacology, Gifu University Graduate School of Medicine, Gifu, 501-1194, Japan
[b] Department of Clinical Laboratory, National Hospital for Geriatric Medicine, National Center for Geriatrics and Gerontology, Obu, Aichi 474-8511, Japan
[c] Department of Biochemistry, Institute for Developmental Research, Aichi Human Service Center, Kasugai 486-0392, Japan

ARTICLE INFO

Article history:
Received 16 November 2007
Accepted 26 February 2008

Keywords:
Catechin
TGF-β
Heat shock protein
Protein kinase
Osteoblast

ABSTRACT

We previously reported that transforming growth factor-β (TGF-β) stimulates heat shock protein 27 (HSP27) induction through p38 mitogen-activated protein (MAP) kinase and extracellular signal-regulated kinase 1/2 (ERK1/2) in osteoblast-like MC3T3-E1 cells. In the present study, we investigated whether (−)-epigallocatechin gallate (EGCG), the major polyphenol found in green tea, affects the TGF-β-stimulated induction of HSP27 in these cells, and its underlying mechanism. EGCG significantly suppressed the HSP27 induction stimulated by TGF-β in a dose-dependent manner between 10 and 30 μM without affecting the HSP70 levels. TGF-β with or without EGCG did not affect the advanced oxidation protein products. The TGF-β-induced phosphorylation of p38 MAP kinase and ERK1/2 was not affected by EGCG. SP600125, a specific inhibitor of stress-activated protein kinase (SAPK)/c-Jun N-terminal kinase (JNK), markedly reduced the HSP27 expression induced by TGF-β. EGCG significantly suppressed the TGF-β-induced phosphorylation of SAPK/JNK without affecting the phosphorylation of Smad2. EGCG attenuated the phosphorylation of both MKK4 and TAK1 induced by TGF-β. These results strongly suggest that EGCG suppresses the TGF-β-stimulated induction of HSP27 via the attenuation of the SAPK/JNK pathway in osteoblasts, and that this effect is exerted at a point upstream from TAK1.

Introduction

Heat shock proteins (HSP) are induced in cells in response to the biological stress such as heat stress and chemical stress (Hendrick and Hartl, 1993). HSPs are classified into high-molecular-weight HSPs such as HSP90 and HSP70, and low-molecular-weight HSPs based on their apparent molecular sizes. Low-molecular-weight HSPs with molecular masses from 10 to 30 kDa, such as HSP27 and αB-crystallin share high homology in amino acid sequences, the "α-crystallin domain" (Benjamin and McMillan, 1998; Inaguma et al., 1993). Though the functions of the low-molecular-weight HSPs are known less than those of the high-molecular-weight HSPs, it is generally believed that they may have chaperoning functions like the high-molecular-weight HSPs (Benjamin and McMillan, 1998; Inaguma et al., 1993). The HSP27 activity has been shown to be regulated by post-translational modification such as phosphorylation (Gaestel et al., 1991; Landry et al., 1992). Under unstimulated conditions, HSP27 exists as a high-molecular weight aggregated form. It is rapidly dissociated as a result of phosphorylation (Kato et al., 1994; Rogalla et al., 1999). The phosphorylation-induced dissociation from the aggregated form correlates with the loss of molecular chaperone activity (Kato et al., 1994; Rogalla et al., 1999). The bone metabolism is regulated by two functional cells, osteoblasts and osteoclasts, responsible for bone formation and bone resorption, respectively (Nijweide et al., 1986). The formation of bone structures and bone remodeling results from the coupling process, bone resorption by activated osteoblasts with subsequent deposition of new matrix by osteoblasts. In osteoblasts, it has been shown that down-regulation of proliferation is accompanied by a transient increase of the HSP27 mRNA expression (Shakoori et al., 1992). In addition, heat-stimulated induction of HSP27 is reportedly facilitated by estrogen (Cooper and Uoshima, 1994). However, the exact role of HSP27 in osteoblasts remains to be clarified.

It is well-known that transforming growth factor-β (TGF-β) regulates cell growth, differentiation and extracellular matrix production (Massague et al., 2000). TGF-β, which is abundantly stored in bone matrix tissue, stimulates the recruitment and proliferation of osteoblasts (Bonewald, 2002). The intracellular signaling of TGF-β is initiated following ligand binding to the TGF-β type II receptor, which activates TGF-β type I receptor (Miyazono et al., 2000). The activated

* Corresponding author. Tel.: +81 58 230 6214; fax: +81 58 230 6215.
E-mail address: okozawa@gifu-u.ac.jp (O. Kozawa).

0024-3205/$ – see front matter © 2008 Published by Elsevier Inc.
doi:10.1016/j.lfs.2008.02.017

type I receptor phosphorylates Smad2 and Smad3, thus resulting in their translocation into the nucleus where they can bind to DNA in the promoters of TGF-β target genes (Miyazono et al., 2001). In addition to the Smad signaling pathway, other signaling pathways such as the mitogen-activated protein (MAP) kinase superfamily have recently been shown to mediate TGF-β signaling (Miyazono et al., 2001). Three major MAP kinases, namely extracellular signal-regulated kinase 1/2 (ERK1/2), p38 MAP kinase, and c-Jun N-terminal kinase, are known to be the central elements used by mammalian cells to transduce the diverse messages (Kyriakis and Avruch, 2001). TGF-β-activated kinase (TAK1), a member of the MAP kinase kinase kinase family, has been identified as an upstream kinase of MAP kinase (Yamaguchi et al., 1995). The kinase activity of TAK1 is stimulated by TGF-β in osteoblast-like MC3T3-E1 cells (Yamaguchi et al., 1995). In our previous study (Hatakeyama et al., 2002), we showed TGF-β to stimulate the induction of HSP27 via p38 MAP kinase and ERK1/2 in osteoblast-like MC3T3-E1 cells. However, the precise roles of the MAP kinase superfamily in the TGF-β signaling system in osteoblasts remain to be clarified.

Compounds in foods such as fruits and vegetables possess beneficial properties for human beings. Among them, flavonoids reportedly show antioxidative, antiproliferative and proapoptotic effects (Jankun et al., 1997; Harbourne and Williams, 2000). Catechins are one of the major flavonoids, which are present in various species of plants such as tea (Harbourne and Williams, 2000). In bone metabolism, catechin has been reported to suppress bone resorption (Delaisse et al., 1986). As for osteoblasts, it has been shown that catechin stimulates alkaline phosphatase activity, a mature osteoblast phenotype and reduces bone-resorptive cytokine production in osteoblast-like MC3T3-E1 cells (Choi and Hwang, 2003). However, the exact role of catechin in osteoblasts has not yet been clarified.

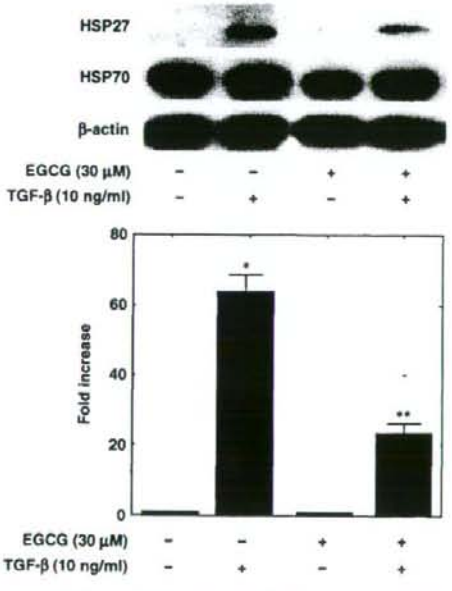

Fig. 1. The effect of EGCG on the TGF-β-stimulated HSP27 induction in MC3T3-E1 cells. The cultured cells were pretreated with 30 μM EGCG for 60 min, and then stimulated with 10 ng/ml TGF-β for 12 h. The extracts of cells were subjected to SDS-PAGE with a subsequent Western blotting analysis with antibodies against HSP27, HSP70 or β-actin. The histogram shows quantitative representations of the levels of TGF-β-induced HSP27 obtained from the laser densitometric analysis of three independent experiments. Each value represents the mean ± SEM of triplicate determinations. Similar results were obtained with two additional and different cell preparations. *$p<0.05$, in comparison to the control. **$p<0.05$, in comparison to the value of TGF-β alone.

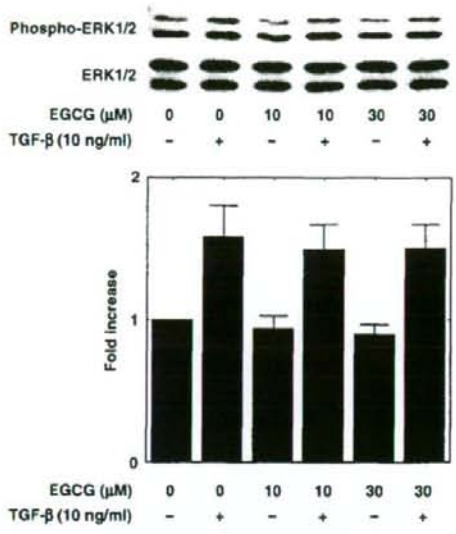

Fig. 2. The effect of EGCG on the TGF-β-induced phosphorylation of ERK1/2 in MC3T3-E1 cells. The cultured cells were pretreated with various doses of EGCG (0, 10, and 30 μM) for 60 min, and then stimulated by 10 ng/ml TGF-β or vehicle for 120 min. The extracts of cells were subjected to SDS-PAGE with a subsequent Western blotting analysis with antibodies against phospho-specific ERK1/2 or ERK1/2. The histogram shows quantitative representations of the levels of TGF-β-induced phosphorylation obtained from the laser densitometric analysis of three independent experiments. Each value represents the mean ± SEM of triplicate determinations. Similar results were obtained with two additional and different cell preparations.

In the present study, we investigated the effect of (−)-epigallocatechin gallate (EGCG), one of the major green tea flavonoids (Harbourne and Williams, 2000), on the TGF-β-stimulated induction of HSP27 and the mechanism in osteoblast-like MC3T3-E1 cells. We herein show that EGCG suppresses the TGF-β-stimulated induction of HSP27 via inhibition of the SAPK/JNK pathway but not the p38 MAP kinase pathway or the ERK1/2 pathway in these cells.

Materials and methods

Materials

TGF-β and HSP27 antibodies were obtained from R&D Systems, Inc. (Minneapolis, MN). β-actin antibodies were purchased from Sigma Chemical Co. (St. Louis, MO). EGCG (>99%) and SP600125 were obtained from Calbiochem-Novabiochem (La Jolla, CA). The advanced oxidation protein products (AOPP) assay kit was obtained from Immunodiagnostic Co., Bensheim, Germany. Phospho-specific ERK1/2 antibodies, ERK1/2 antibodies, phospho-specific p38 MAP kinase antibodies, p38 MAP kinase antibodies, phospho-specific SAPK/JNK antibodies, SAPK/JNK antibodies, phospho-specific Smad2 antibodies, Smad2 antibodies, phospho-specific MKK4 antibodies, MKK4 antibodies, phospho-specific TAK1 antibodies and TAK1 antibodies were purchased from Cell Signaling Technology, Inc. (Beverly, MA). An ECL Western blotting detection system was obtained from Amersham Japan (Tokyo, Japan). All other materials and chemicals were obtained from commercial sources. SP600125 was dissolved in dimethyl sulfoxide. The maximum concentration of dimethyl sulfoxide was 0.1%, which did not affect the Western blot analysis.

Cell culture

Cloned osteoblast-like MC3T3-E1 cells derived from newborn mouse calvaria (Sudo et al., 1983) were maintained as previously

described (Kozawa et al., 1997). Briefly, the cells were cultured in α-minimum essential medium (α-MEM) containing 10% fetal calf serum (FCS) at 37 °C in a humidified atmosphere of 5% CO_2/95% air. The cells were seeded into 90-mm diameter dishes (25×10^4/dish) in α-MEM containing 10% FCS. After 5 days, the medium was exchanged for α-MEM containing 0.3% FCS. The cells were used for experiments after 48 h. When indicated, the cells were pretreated with various doses of EGCG (0, 10 and 30 μM).

Western blot analysis

The cultured cells were stimulated by 10 ng/ml TGF-β or vehicle in serum-free α-MEM for the indicated periods. The cells were washed twice with phosphate-buffered saline and then lysed, homogenized, sonicated, and immediately boiled in a lysis buffer containing 62.5 mM Tris/Cl, pH 6.8, 2% sodium dodecyl sulfate (SDS), 50 mM dithiothreitol, and 10% glycerol. The sample was used for the analysis by Western blotting. SDS-polyacrylamide gel electrophoresis (PAGE) was performed by the method of Laemmli (1970) in 10% polyacrylamide gel. The Western blot analysis was performed as described previously (Kato et al., 1996), using HSP27 antibodies, β-actin antibodies, phospho-specific ERK1/2 antibodies, ERK1/2 antibodies, phospho-specific p38 MAP kinase antibodies, p38 MAP kinase antibodies, phospho-specific SAPK/JNK antibodies, SAPK/JNK antibodies, phospho-specific Smad2 antibodies, Smad2 antibodies, phospho-specific MKK4 antibodies, MKK4 antibodies, phospho-specific TAK1 antibodies or TAK antibodies, with peroxidase-labeled antibodies raised in goat against rabbit IgG being used as second antibodies. The peroxidase activity on PVDF membranes was visualized on X-ray film by means of the ECL Western blotting detection system and it was quantitated using the NIH image software program. All of the Western blot analyses were repeated at least three times in independent experiments.

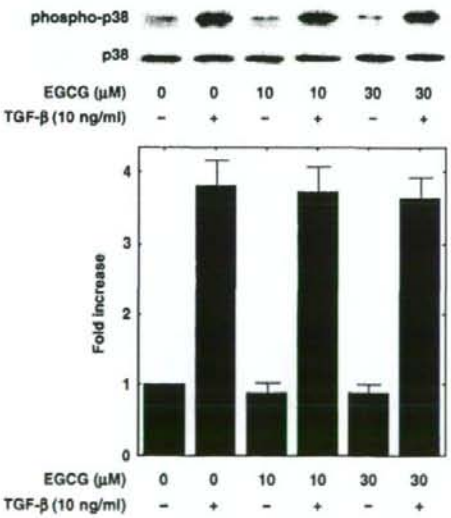

Fig. 3. The effect of EGCG on the TGF-β-induced phosphorylation of p38 MAP kinase in MC3T3-E1 cells. The cultured cells were pretreated with various doses of EGCG (0, 10, and 30 μM) for 60 min, and then stimulated by 10 ng/ml TGF-β or vehicle for 120 min. The extracts of cells were subjected to SDS-PAGE with a subsequent Western blotting analysis with antibodies against phospho-specific p38 MAP kinase or p38 MAP kinase. The histogram shows quantitative representations of the levels of TGF-β-induced phosphorylation obtained from the laser densitometric analysis of three independent experiments. Each value represents the mean ± SEM of triplicate determinations. Similar results were obtained with two additional and different cell preparations.

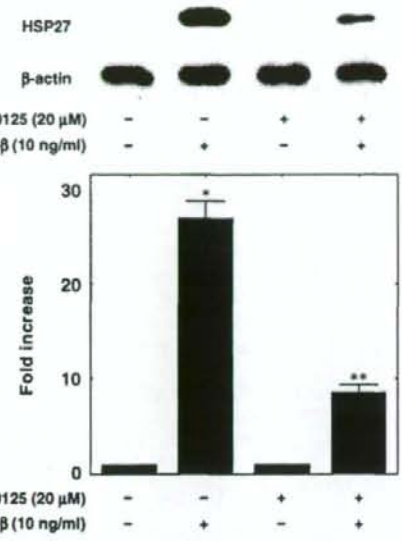

Fig. 4. The effect of SP600125 on the TGF-β-stimulated HSP27 induction in MC3T3-E1 cells. The cultured cells were pretreated with 20 μM SP600125 for 60 min, and then stimulated with 10 ng/ml TGF-β or vehicle for 12 h. The extracts of cells were subjected to SDS-PAGE with a subsequent Western blotting analysis with antibodies against HSP27 or β-actin. The histogram shows quantitative representations of the levels of TGF-β-induced HSP27 obtained from the laser densitometric analysis of three independent experiments. Each value represents the mean ± SEM of triplicate determinations. Similar results were obtained with two additional and different cell preparations. *$p<0.05$, in comparison to the control. **$p<0.05$, in comparison to the value of TGF-β alone.

AOPP assay

The cultured cells were pretreated with various doses of EGCG (0, 10 and 30 μM) for 60 min, and then stimulated by 10 ng/ml TGF-β or vehicle for 12 h. The cell lysates were prepared according to the manufacture's instructions, and the AOPP contents of cell lysates were measured using an AOPP assay kit.

Statistical analysis

The data were analyzed by ANOVA followed by the Bonferroni method for multiple comparisons between pairs, and a $p<0.05$ was considered significant. All data are presented as the mean ± SEM of triplicate determinations.

Results

Effect of EGCG on the TGF-β-stimulated HSP27 induction in MC3T3-E1 cells

We examined the effect of EGCG on the TGF-β-stimulated induction of HSP27. EGCG significantly reduced the TGF-β-induced levels of HSP27 (Fig. 1). EGCG (30 μM) caused about 60% reduction in the TGF-β-effect. We have previously shown that TGF-β does not affect the levels of HSP70, a high-molecular-weight HSP, in osteoblast-like MC3T3-E1 cells (Hatakeyama et al., 2002). EGCG had little effect on the levels of HSP70 (Fig. 1). We confirmed that the viability of the cells incubated at 37 °C for 24 h in the presence of 30 μM EGCG was more than 90% in comparison to that of the control cells (Tokuda et al., in press).

Effect of TGF-β with or without EGCG on AOPP contents in MC3T3-E1 cells

It is well-known that flavonoids show an antioxidative effect (Jankun et al., 1997; Harbourne and Williams, 2000). To clarify whether the antioxidative effect is involved in the suppression by EGCG of HSP27

induction stimulated by TGF-β, we investigated the effect of TGF-β on the formation of AOPP with or without EGCG in osteoblast-like MC3T3-E1 cells. TGF-β, with or without EGCG had no effect on the AOPP contents (not detectable under the experimental condition at all; <0.044 mM Trox).

Effects of EGCG on the TGF-β-stimulated phosphorylation of ERK1/2 and p38 MAP kinase in MC3T3-E1 cells

In our previous study (Hatakeyama et al., 2002), we demonstrated that the activation of ERK1/2 and p38 MAP kinase at least in part mediate the TGF-β-stimulated induction of HSP27 in osteoblast-like MC3T3-E1 cells. Therefore, we next examined the effect of EGCG on the TGF-β-stimulated phosphorylation of ERK1/2. However, EGCG did not affect the TGF-β-induced phosphorylation of ERK1/2 in MC3T3-E1 cells (Fig. 2).

In addition, EGCG failed to influence the TGF-β-induced phosphorylation of p38 MAP kinase (Fig. 3).

Effect of EGCG on the TGF-β-induced phosphorylation of SAPK/JNK in MC3T3-E1 cells

It is generally recognized that SAPK/JNK is one of the MAP kinase superfamily (Kyriakis and Avruch, 2001). We have previously reported that SAPK/JNK plays a role in the TGF-β-stimulated synthesis of vascular endothelial growth factor in osteoblast-like MC3T3-E1 cells (Kanno et al., 2005). In order to investigate whether SAPK/JNK is involved in the EGCG-induced suppression of HSP27 induction in MC3T3-E1 cells, we next examined the effect of SP600125, a highly specific inhibitor of SAPK/JNK (Bennett et al., 2001), on the TGF-β-stimulated HSP27 induction. SP600125 markedly suppressed the levels of TGF-β-induced HSP27 (Fig. 4).

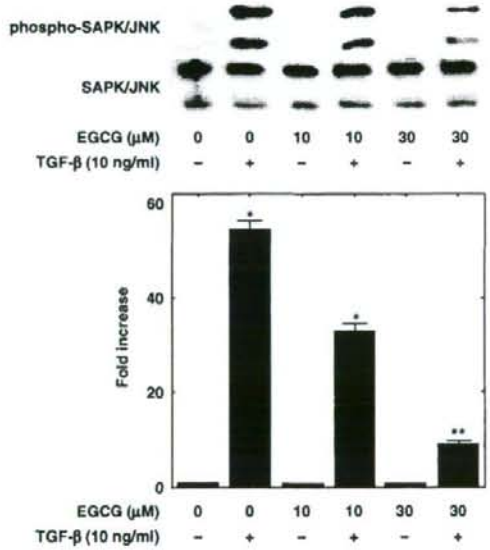

Fig. 5. The effect of EGCG on the TGF-β-induced phosphorylation of SAPK/JNK in MC3T3-E1 cells. The cultured cells were pretreated with various doses of EGCG (0, 10, and 30 μM) for 60 min, and then stimulated by 10 ng/ml TGF-β or vehicle for 120 min. The extracts of cells were subjected to SDS-PAGE with a subsequent Western blotting analysis with antibodies against phospho-specific SAPK/JNK or SAPK/JNK. The histogram shows quantitative representations of the levels of TGF-β-induced phosphorylation obtained from the laser densitometric analysis of three independent experiments. Each value represents the mean ± SEM of triplicate determinations. Similar results were obtained with two additional and different cell preparations. *$p<0.05$, in comparison to the control. **$p<0.05$, in comparison to the value of TGF-β alone.

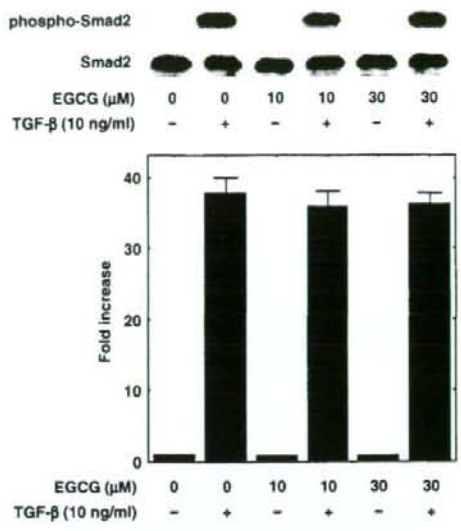

Fig. 6. The effect of EGCG on the TGF-β-induced phosphorylation of Smad2 in MC3T3-E1 cells. The cultured cells were pretreated with various doses of EGCG (1, 10, and 30 μM) for 60 min, and then stimulated by 10 ng/ml TGF-β or vehicle for 120 min. The extracts of cells were subjected to SDS-PAGE with a subsequent Western blotting analysis with antibodies against phospho-specific Smad2 or Smad2. The histogram shows quantitative representations of the levels of TGF-β-induced phosphorylation obtained from the laser densitometric analysis of three independent experiments. Each value represents the mean ± SEM of triplicate determinations. Similar results were obtained with two additional and different cell preparations.

In order to clarify whether the SAPK/JNK pathway is involved in the suppressive effect of EGCG on the HSP27 induction, we examined the effect of EGCG on the TGF-β-induced phosphorylation of SAPK/JNK.

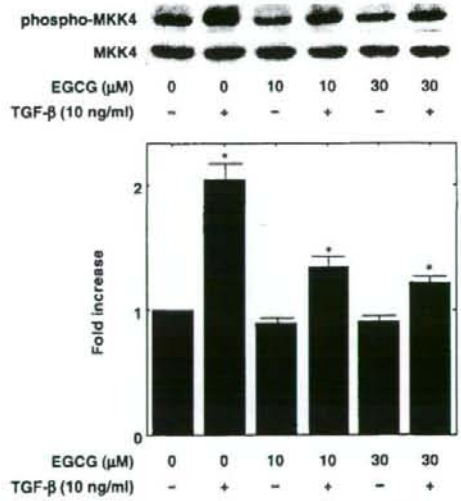

Fig. 7. The effect of EGCG on the TGF-β-induced phosphorylation of MKK4 in MC3T3-E1 cells. The cultured cells were pretreated with various doses of EGCG (1, 10, and 30 μM) for 60 min, and then stimulated by 10 ng/ml TGF-β or vehicle for 120 min. The extracts of cells were subjected to SDS-PAGE with a subsequent Western blotting analysis with antibodies against phospho-specific MKK4 or MKK4. The histogram shows quantitative representations of the levels of TGF-β-induced phosphorylation obtained from the laser densitometric analysis of three independent experiments. Each value represents the mean ± SEM of triplicate determinations. Similar results were obtained with two additional and different cell preparations. *$p<0.05$, in comparison to the control. **$p<0.05$, in comparison to the value of TGF-β alone.

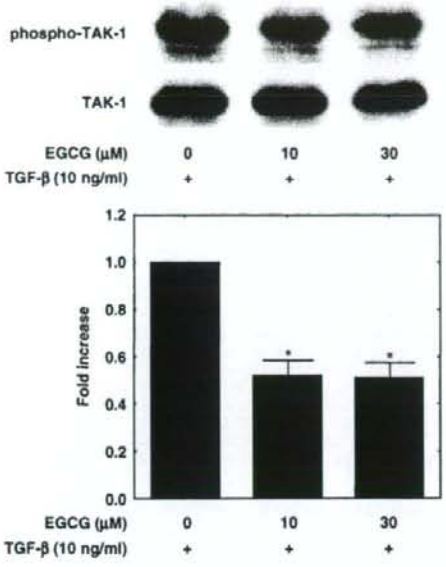

Fig. 8. The effect of EGCG on the TGF-β-induced phosphorylation of TAK1 in MC3T3-E1 cells. The cultured cells were pretreated with various doses of EGCG (1, 10, and 30 μM) for 60 min, and then stimulated by 10 ng/ml TGF-β for 120 min. The extracts of cells were subjected to SDS-PAGE with a subsequent Western blotting analysis with antibodies against phospho-specific TAK1 or TAK1. The histogram shows quantitative representations of the levels of TGF-β-induced phosphorylation obtained from the laser densitometric analysis of three independent experiments. Each value represents the mean±SEM of triplicate determinations. Similar results were obtained with two additional and different cell preparations. *$p<0.05$, in comparison to the value of TGF-β alone.

EGCG significantly attenuated the TGF-β-induced phosphorylation of SAPK/JNK in a dose-dependent manner (Fig. 5). EGCG (30 μM) caused about an 80% reduction in the TGF-β-effect.

Effect of EGCG on the TGF-β-induced phosphorylation of Smad2 in MC3T3-E1 cells

It is well-known that TGF-β employs Smad proteins such as Smad2 and Smad3 as the intracellular mediator of signaling (Miyazono et al., 2000). We therefore additionally examined the effect of EGCG on the TGF-β-induced activation of Smad2. However, EGCG had no effect on the TGF-β-induced phosphorylation of Smad2 (Fig. 6). Therefore, it seems unlikely that EGCG acts at a point upstream of Smad2 in these cells.

Effects of EGCG on the TGF-β-induced phosphorylation of MKK4 and TAK1 in MC3T3-E1 cells

It is generally recognized that SAPK/JNK is regulated by the upstream kinases, MKK4 as MAP kinase kinase and TAK1 as MAP kinase kinase kinase in the signaling of TGF-β (Yamaguchi et al., 1995). We thus further examined the effects of EGCG on the phosphorylation of MKK4 and TAK1 induced by TGF-β in osteoblast-like MC3T3-E1 cells. EGCG significantly reduced the phosphorylation of MKK4 induced by TGF-β (Fig. 7). TGF-β-induced phosphorylation of TAK1 was also attenuated by EGCG (Fig. 8). It is likely that EGCG regulates TGF-β-stimulated SAPK/JNK activation at a point upstream from TAK1.

Discussion

In the present study, we first demonstrated that EGCG significantly suppressed the TGF-β-stimulated induction of HSP27, a low-molecular-weight HSP, in osteoblast-like MC3T3-E1 cells. We found that TGF-β with or without EGCG had no effect on the AOPP contents. It therefore seems unlikely that oxidative damage is induced by TGF-β under the experimental condition or that the antioxidative effect of EGCG is involved in the reduction of TGF-β-stimulated HSP27 induction in osteoblasts. In addition, the level of HSP70 has also been reported to be very high also in the control group without TGF-β. As a result, it seems that HSP70 plays a role as a house-keeping molecule in osteoblast-like cells.

We next investigated the mechanism of EGCG underlying the inhibitory effect on the TGF-β-stimulated HSP27 induction. It is well recognized that the MAP kinase superfamily plays an important role in a variety of cellular functions including proliferation, differentiation, and cell death in various cells (Kyriakis and Avruch, 2001). Three major MAP kinases such as ERK1/2, p38 MAP kinase and SAPK/JNK are known to be central elements used by mammalian cells to transduce the diverse messages. We have previously shown that ERK1/2 and p38 MAP kinase act as positive regulators in the TGF-β-stimulated induction of HSP27 in osteoblast-like MC3T3-E1 cells (Hatakeyama et al., 2002). In the present study, EGCG failed to affect the TGF-β-induced phosphorylation of ERK1/2. In addition, EGCG had little effect on the TGF-β-induced phosphorylation of p38 MAP kinase. Taking our findings into account, it seems unlikely that the EGCG-induced suppression of TGF-β-stimulated induction of HSP27 is due to the inhibition of ERK1/2 and p38 MAP kinase in osteoblast-like MC3T3-E1 cells.

SAPK/JNK is a member of the MAP kinase superfamily in addition to ERK1/2 and p38 MAP kinase (Kyriakis and Avruch, 2001). Therefore, we next investigated the correlation between the EGCG-induced inhibition of HSP27 levels and SAPK/JNK in osteoblast-like MC3T3-E1 cells. We have already reported that TGF-β stimulates the activation of SAPK/JNK in these cells (Kanno et al., 2005). In the present study, we showed that the TGF-β-stimulated levels of HSP27 were significantly reduced by SP600125 (Bennett et al., 2001). Therefore, these results suggest that SAPK/JNK is involved in the TGF-β-stimulated levels of HSP27 in these cells. In addition, EGCG markedly suppressed the TGF-β-induced phosphorylation of SAPK/JNK. Taking our findings into account, it is most likely that the inhibition by EGCG in the TGF-β-stimulated induction of HSP27 is mediated through the suppression of the SAPK/JNK pathway in the osteoblast-like MC3T3-E1 cells. On the other hand, we herein showed that EGCG hardly affected the TGF-β-induced Smad2 phosphorylation, suggesting that EGCG does not act at a point upstream of Smad2-mediated signaling in osteoblasts. We furthermore found that EGCG significantly reduced the phosphorylation of both MKK4 and TAK1 induced by TGF-β in these cells. Based on our findings, it is most likely that EGCG regulates TGF-β-stimulated SAPK/JNK activation at a point upstream from TAK1.

Osteoporosis is one of the major problems regarding the health of elderly persons in the advanced countries. It is recognized that tea drinkers appear to have a low risk of osteoporosis (Siddiqui et al., 2004). Catechin is one of the major flavonoids contained in various species of plants including tea (Harbourne and Williams, 2000). Regarding the bone metabolism, catechin has been reported to suppress bone resorption (Delaisse et al., 1986). As for osteoblasts, it has been shown that catechin stimulates alkaline phosphatase activity, a mature osteoblast phenotype, and reduces bone-resorptive cytokine production in osteoblast-like MC3T3-E1 cells (Choi and Hwang, 2003). Taking our present findings into account, catechin could therefore affect the osteoblast function through the modulation of HSP27 induction stimulated by the local factors, such as TGF-β resulting in the modulation of bone metabolism toward the beneficial for prevention of bone loss.

On the other hand, the pharmacokinetics of EGCG in human volunteers taking a single dosage of 1600 mg/day showed a rapid absorption, with a maximum plasma concentration value of 11.08 μM (=3392 ng/ml); the time to reach maximum plasma concentration was 2.2 h, and the terminal elimination half-life ranged between 1.9 and

4.6 h (Ullmann et al., 2003). Moreover, it has been reported that 10-day repeated administration of oral doses of EGCG of up to 800 mg/day is safe and well tolerated (Ullmann et al., 2004). We herein showed that the inhibitory effect of EGCG on TGF-β-stimulated HSP27 induction was significantly observed at 10 μM. It is thus probable that the concentration of EGCG physiologically reaches that which promotes the effect shown here. In addition, the plasma concentration of EGCG required for cancer prevention or anti-inflammatory effects has been shown to range from over 10 μM to 50 μM (Lambert and Yang, 2003; Wheeler et al., 2004; Aktas et al., 2004). In regard to the efficacy of EGCG, our present findings seem to be consistent with these previous observations. Although the physiological significance of HSP27 in osteoblasts has not yet been clarified, it is probable that EGCG-induced suppression of the SAPK/JNK pathway plays a pivotal effect on bone metabolism via reducing the levels of HSP27 in osteoblasts. Our present findings are thus considered to provide new insight into the pharmacological effects of catechin on bone metabolism. Further investigations are needed to elucidate the precise role of catechin in the bone metabolism.

Conclusion

Our present results strongly suggest that EGCG reduces the TGF-β-stimulated induction of HSP27 via the suppression of the SAPK/JNK pathway in osteoblasts, and that this effect is exerted at a point upstream from TAK1.

Acknowledgements

We are very grateful to Yoko Kawamura for her skillful technical assistance. This work was supported in part by Grants-in-Aid for Scientific Research (Nos. 16590873 and 16591482) for the Ministry of Education, Science, Sports and Culture of Japan, the Research Grants for Longevity Sciences [15A-1 and 15C-2], Research on Proteomics and Research on Fracture and Dementia from Ministry of Health, Labour and Welfare of Japan.

References

Aktas, O., Prozorovski, T., Smorodchenko, A., Savaskan, N.E., Lauster, R., Kloetzel, P.M., Infante-Duarte, C., Brocke, S., Zipp, F., 2004. Green tea epigallocatechin-3-gallate mediates T cellular NF-kappa B inhibition and exerts neuroprotection in autoimmune encephalomyelitis. Journal of Immunology 173, 5794–5800.

Benjamin, I.J., McMillan, D.R., 1998. Stress (heat shock) proteins: molecular chaperones in cardiovascular biology and disease. Circulation Research 83, 117–132.

Bennett, B.L., Sasaki, D.T., Murray, B.W., O'Leary, E.C., Sakata, S.T., Xu, W., Leisten, J.C., Motiwala, A., Pierce, S., Satoh, Y., Bhagwat, S.S., Manning, A.M., Anderson, D.W., 2001. SP600125, an anthrapyrazolone inhibitor of Jun N-terminal kinase. Proceedings of the National Academy of Sciences of the United States of America 98, 13681–13686.

Bonewald, L.F., 2002. Transforming growth factor-β. In: Bilezikian, J.P., Raisz, L.G., Rodan, G.A. (Eds.), Principles of Bone Biology, 2nd ed. Academic Press, San Diego, pp. 903–918.

Choi, E.-M., Hwang, J.-K., 2003. Effects of (+)-catechin on the function of osteoblastic cells. Biological & Pharmacological Bulletin 26, 523–526.

Cooper, L.F., Uoshima, K., 1994. Differential estrogenic regulation of small M(r) heat shock protein expression in osteoblasts. Journal of Biological Chemistry 269, 7869–7873.

Delaisse, J.M., Eeckhout, Y., Vaes, G., 1986. Inhibition of bone resorption in culture by (+)-catechin. Biochemical Pharmacology 35, 3091–3094.

Gaestel, M., Schroder, W., Benndorf, R., Lippmann, C., Buchner, K., Hucho, F., Erdmann, V.A., Bielka, H., 1991. Identification of the phosphorylation sites of the murine small heat shock protein hsp25. Journal of Biological Chemistry 266, 14721–14724.

Harbourne, J.B., Williams, C.A., 2000. Advances in flavonoid research since 1992. Phytochemistry 55, 481–504.

Hatakeyama, D., Kozawa, O., Niwa, M., Matsuno, H., Ito, H., Kato, K., Tatematsu, N., Shibata, T., Uematsu, T., 2002. Upregulation by retinoic acid of TGF-β-stimulated heat shock protein 27 induction in osteoblasts: involvement of mitogen-activated protein kinases. Biochimica et Biophysica Acta 1589, 15–30.

Hendrick, J.P., Hartl, F.U., 1993. Molecular chaperone functions of heat-shock proteins. Annual Review of Biochemistry 62, 349–384.

Inaguma, Y., Goto, S., Shinohara, H., Hasegawa, K., Ohshima, K., Kato, K., 1993. Physiological and pathological changes in levels of the two small stress proteins, HSP27 and alpha B crystallin, in rat hindlimb muscles. Journal of Biochemistry (Tokyo) 114, 378–384.

Jankun, J., Selman, S.H., Swiercz, R., Skrzypczak-Jankun, E., 1997. Why drinking green tea could prevent cancer. Nature 387, 561.

Kanno, Y., Ishisaki, A., Yoshida, M., Tokuda, H., Numata, O., Kozawa, O., 2005. SAPK/JNK plays a role in transforming growth factor-β-induced VEGF synthesis in osteoblasts. Hormone and Metabolic Research 37, 140–145.

Kato, K., Hasegawa, K., Goto, S., Inaguma, Y., 1994. Dissociation as a result of phosphorylation of an aggregated form of the small stress protein, hsp27. Journal of Biological Chemistry 269, 11274–11278.

Kato, K., Ito, H., Hasegawa, K., Inaguma, Y., Kozawa, O., Asano, T., 1996. Modulation of the stress-induced synthesis of hsp27 and alpha B-crystallin by cyclic AMP in C6 rat glioma cells. Journal of Neurochemistry 66, 946–950.

Kozawa, O., Suzuki, A., Tokuda, H., Uematsu, T., 1997. Prostaglandin $F_{2\alpha}$ stimulates interleukin-6 synthesis via activation of PKC in osteoblast-like cells. American Journal of Physiology 272, E208–E211.

Kyriakis, J.M., Avruch, J., 2001. Mammalian mitogen-activated protein kinase signal transduction pathways activated by stress and inflammation. Physiological Reviews 81, 807–869.

Laemmli, U.K., 1970. Cleavage of structural proteins during the assembly of the head of bacteriophage T4. Nature 227, 680–685.

Lambert, J.D., Yang, C.S., 2003. Mechanisms of cancer prevention by tea constituents. Journal of Nutrition 133, 3262S–3267S.

Landry, J., Lambert, H., Zhou, M., Lavoie, J.N., Hickey, E., Weber, L.A., Anderson, C.W., 1992. Human HSP27 is phosphorylated at serines 78 and 82 by heat shock and mitogen-activated kinases that recognize the same amino acid motif as S6 kinase II. Journal of Biological Chemistry 267, 794–803.

Massague, J., Blain, S.W., Lo, R.S., 2000. TGF-β signaling in growth control, cancer, and heritable disorders. Cell 103, 295–309.

Miyazono, K., ten Dijke, P., Heldin, C.H., 2000. TGF-β signaling by Smad proteins. Advances in Immunology 75, 115–157.

Miyazono, K., Kusanagi, K., Inoue, H., 2001. Divergence and convergence of TGF-β/BMP signaling. Journal of Cellular Physiology 187, 265–276.

Nijweide, P.J., Burger, E.H., Feyen, J.H.M., 1986. Cells of bone: proliferation, differentiation, and hormonal regulation. Physiological Reviews 86, 855–886.

Rogalla, T., Ehrnsperger, M., Preville, X., Kotlyarov, A., Lutsch, G., Ducasse, C., Paul, C., Wieske, M., Arrigo, A.P., Buchner, J., Gaestel, M., 1999. Regulation of Hsp27 oligomerization, chaperone function, and protective activity against oxidative stress/tumor necrosis factor a by phosphorylation. Journal of Biological Chemistry 274, 18947–18956.

Shakoori, A.R., Oberdorf, A.M., Owen, T.A., Weber, L.A., Hickey, E., Stein, J.L., Lian, J.B., Stein, G.S., 1992. Expression of heat shock genes during differentiation of mammalian osteoblasts and promyelocytic leukemia cells. Journal of Cellular Biochemistry 48, 277–287.

Siddiqui, I.A., Afaq, F., Adhami, V.M., Ahmad, N., Mukhtar, H., 2004. Antioxidants of the beverage tea in promotion of human health. Antioxidants & Redox Signalling 6, 571–582.

Sudo, H., Kodama, H., Amagai, Y., Yamamoto, S., Kasai, S., 1983. *In vitro* differentiation and calcification in a new clonal osteogenic cell line derived from newborn mouse calvaria. Journal of Cell Biology 96, 191–198.

Tokuda, H., Takai, S., Hanai, Y., Matsushima-Nishiwaki, R., Yamauchi, J., Harada, A., Hosoi, T., Ohta, T., Kozawa, O., in press. (−)-Epigallocatechin gallate inhibits basic fibroblast growth factor-induced interleukin-6 synthesis in osteoblasts. Hormone and Metabolic Research.

Ullmann, U., Haller, J., Decourt, J.P., Girault, N., Girault, J., Richard-Caudron, A.S., Pineau, B., Weber, P., 2003. A single ascending dose study of epigallocatechin gallate in healthy volunteers. Journal of International Medical Research 31, 88–101.

Ullmann, U., Haller, J., Decourt, J.D., Girault, J., Spitzer, V., Weber, P., 2004. Plasma-kinetic characteristics of purified and isolated green tea catechin epigallocatechin gallate (EGCG) after 10 days repeated dosing in healthy volunteers. International Journal for Vitamin and Nutrition Research 74, 269–278.

Wheeler, D.S., Catravas, J.D., Odoms, K., Denenberg, A., Malfotra, V., Wong, H.R., 2004. Epigallocatechin-3-gallate, a green tea-derived polyphenol, inhibits IL-1 beta-dependent proinflammatory signal transduction in cultured respiratory epithelial cells. Journal of Nutrition 134, 1039–1044.

Yamaguchi, K., Shirakabe, K., Shibuya, H., Irie, K., Oishi, I., Ueno, N., Taniguchi, T., Nishida, E., Matsumoto, K., 1995. Identification of a member of the MAPKKK family as a potential mediator of TGF-β signal transduction. Science 270, 2008–2011.

Archives of Biochemistry and Biophysics 475 (2008) 80–86

Contents lists available at ScienceDirect

Archives of Biochemistry and Biophysics

journal homepage: www.elsevier.com/locate/yabbi

HSP27 phosphorylation is correlated with ADP-induced platelet granule secretion

Hisaaki Kato [a,b], Shinji Takai [a], Rie Matsushima-Nishiwaki [a], Seiji Adachi [a], Chiho Minamitani [d], Takanobu Otsuka [d], Haruhiko Tokuda [a,c], Shigeru Akamatsu [e], Tomoaki Doi [a,b], Shinji Ogura [b], Osamu Kozawa [a,*]

[a] Department of Pharmacology, Gifu University Graduate School of Medicine, Yanagido 1-1, Gifu 501-1194, Japan
[b] Department of Emergency and Disaster Medicine, Gifu University Graduate School of Medicine, Gifu, Japan
[c] Department of Clinical Laboratory, National Hospital for Geriatric Medicine, National Center for Geriatrics and Gerontology, Obu, Aichi, Japan
[d] Department of Orthopedic Surgery, Nagoya City University Graduate School of Medical Sciences, Nagoya, Aichi, Japan
[e] Department of Intensive Care Medicine, Matsunami General Hospital, Gifu, Japan

ARTICLE INFO

Article history:
Received 1 February 2008
and in revised form 16 April 2008
Available online 29 April 2008

Keywords:
HSP27
Platelet
Phosphorylation
ADP
Granule secretion

ABSTRACT

Adenosine diphosphate (ADP) plays a crucial role in hemostasis and thrombosis by activating platelets. ADP has been reported to induce heat-shock protein (HSP) 27 phosphorylation in human platelets. However, the exact role of HSP27 phosphorylation in human platelets has not yet been clarified. In the present study, we investigated the mechanisms and the roles of ADP-induced HSP27 phosphorylation in human platelets. We showed for the first time that both of decreased phosphorylation levels of HSP27 by PD98059, a MEK1/2 inhibitor and SB203580, a p38 MAPK inhibitor were correlated with the suppressed levels of platelet granule secretion but not with platelet aggregation. Furthermore, the inhibition of either the p44/p42 MAPK or p38 MAPK pathways had no effect on ADP-induced platelet aggregation. These results strongly suggest that the ADP-induced phosphorylation of HSP27 via p44/p42 MAPK and/or p38 MAPK is therefore sufficient for platelet granule secretion but not for platelet aggregation in humans.

Platelet aggregation and activation represent the first step in thrombogenesis. Platelet aggregation plays a central role in the development of thrombus formation. Thrombus formation is induced by several agonists that provoke platelet granule secretion and aggregation. Platelets are reactive to various stimuli and release the materials stored in the three specific granules; dense granules, α-granules and lysosomes. Three specific granule populations store different types of constituents. Dense granules contain small non-protein molecules such as serotonin (5-HT) and adenosine diphosphate (ADP)[1] [1]. α-Granules contain large adhesive and healing proteins such as platelet-derived growth factor (PDGF) and von Willebrand factor [1]. However, the detailed mechanism of platelet granule secretion is not precisely known.

One of the most important and potent agonists, ADP, activates platelets through P2-receptors [2,3]. The currently available antiplatelet agents, such as aspirin, show clinical efficacy in the treatment of arterial thrombotic disorders by inhibiting platelet aggregation [4,5]. ADP is considered to be a weak agonist by itself in comparison, for example, with thrombin or collagen [6]; however, ADP is a necessary cofactor for the normal activation of platelets by other agonists. Low concentrations of ADP potentiate or amplify the effects of an agonist for platelet activation [7]. It was recently reported that the activation of P2-receptors lead to both platelet aggregation and shape change and that P2Y1 or P2Y12 receptor activation by ADP results in the activation of p38 mitogen-activated protein kinase (MAPK) or p44/p42 MAPK, respectively, in human platelet [8,9].

Heat-shock proteins (HSPs) are expressed in both prokaryotic and eukaryotic cells in response to various types of biological stress, such as heat and chemical stress [10]. HSPs are classified into high-molecular-weight HSPs and low-molecular-weight HSPs based on their apparent molecular sizes. Low-molecular-weight HSPs with molecular masses from 10 to 30 kDa, such as HSP27 and αB-crystallin have high homology in their amino acid sequences [11,12]. Though less is known about the functions of the low-molecular-weight HSPs than those of the high-molecular-weight HSPs, it is generally accepted that they may have chaperoning functions like the high-molecular-weight HSPs [11,12]. HSP27 becomes rapidly phosphorylated in response to various stresses, as well as to exposure to cytokines and mitogens [13,14]. It is recognized that HSP27 activity is regulated by post-translational modifications such as phosphorylation [11,15]. Human HSP27 is phosphorylated at three serine residues (Ser-15, Ser-78, and Ser-82), whereas mouse HSP27 is phosphorylated at two serine

* Corresponding author. Fax: +81 58 230 6215.
E-mail address: okozawa@gifu-u.ac.jp (O. Kozawa).

[1] *Abbreviations used:* ADP, adenosine diphosphate; PDGF, platelet-derived growth factor; MAPK, mitogen-activated protein kinase; HSPs, heat-shock proteins; SAPK/JNK, phospho-stress-activated protein kinase/c-*Jun N*-terminal kinase; PRP, platelet-rich plasma; PVDF, Immobilion-P membrane.

0003-9861/$ - see front matter © 2008 Elsevier Inc. All rights reserved.
doi:10.1016/j.abb.2008.04.023

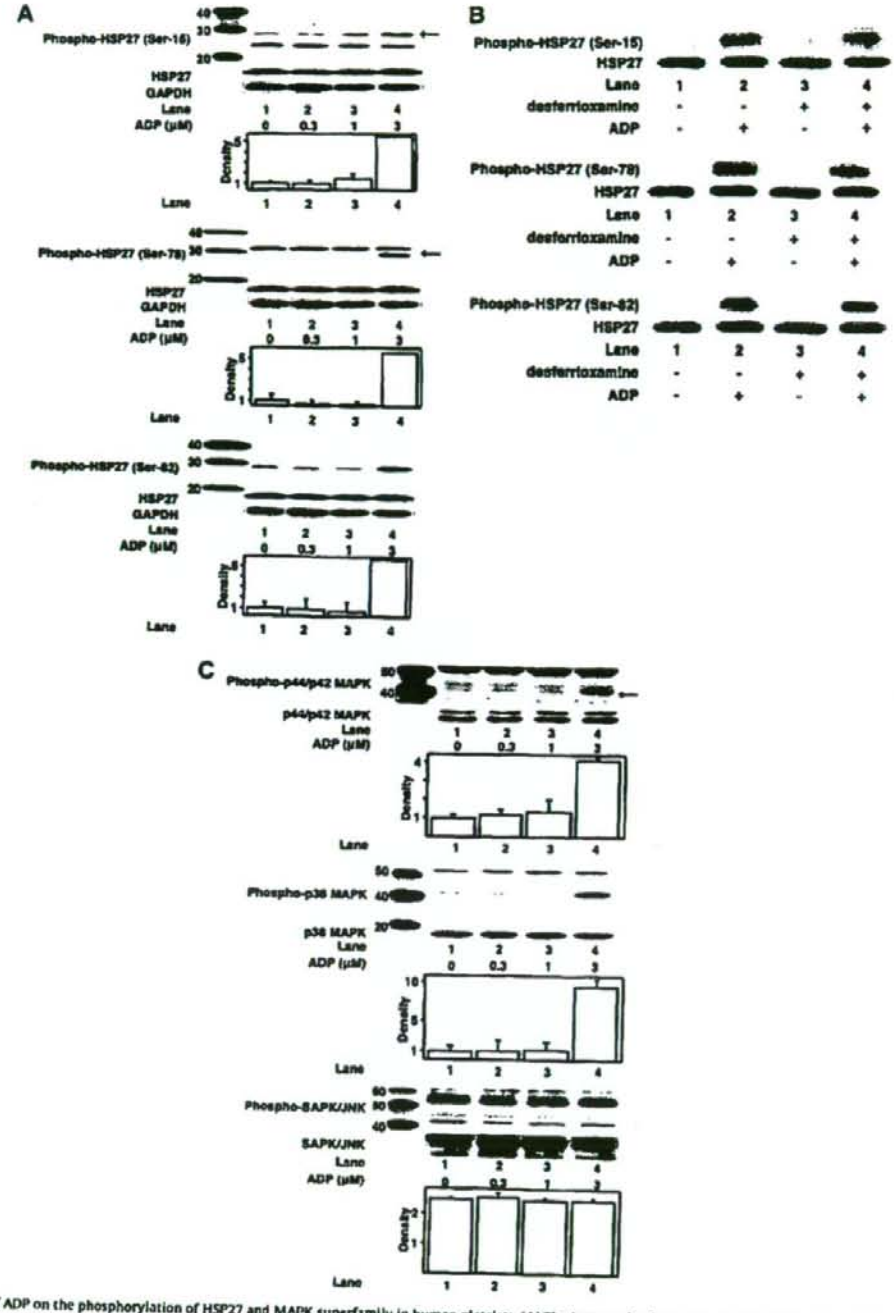

Fig. 1. Effects of ADP on the phosphorylation of HSP27 and MAPK superfamily in human platelets. (A) The human platelets were stimulated by either saline or various doses of ADP in an aggregometer at 37 °C for 5 min with a stirring speed of 800 rpm. Aggregation was terminated by the addition of an ice-cold EDTA (10 mM) solution. The extracts of cells were subjected to SDS–PAGE using antibodies against total HSP27, phospho-specific HSP27 (Ser-15, Ser-78, and Ser-82) and GAPDH. (B) The human platelets were pretreated with or without 2 mM of desferrioxiamine for 15 min before ADP stimulation. After stimulation with 3 mM of ADP for 4 min, platelet aggregation was then terminated by the addition of an ice-cold EDTA (10 mM) solution. The extracts of cells were then subjected to SDS–PAGE using antibodies against total HSP27 and phospho-specific HSP27 (Ser-15, Ser-78, and Ser-82). (C) The extracts of cells were subjected to SDS–PAGE using antibodies against phospho-specific p44/p42 MAPK, p44/p42 MAPK, phospho-specific p38 MAPK, p38 MAPK, phospho-specific SAPK/JNK, SAPK/JNK, and GAPDH. Lower graph shows the quantification data of the amount of the indicated protein shown in the upper figures. Representative results from at least three independent experiments are shown.

residues (Ser-15 and Ser-82) [11]. Under unstimulated conditions, HSP27 exists in a high-molecular-weight aggregated form. It is rapidly dissociated as a result of phosphorylation [16,17]. The phosphorylation-induced dissociation from the aggregated form correlates with the loss of molecular chaperone activity [16,17]. ADP has been reported to induce HSP27 phosphorylation in human platelets [18]. In addition, it has been shown that HSP27 phosphorylation is catalyzed by the MAPK superfamily such as p38 MAPK, phospho-stress-activated protein kinase/c-*Jun N*-terminal kinase (SAPK/JNK) and p44/p42 MAPK [11,19,20]. However, the exact role of HSP27 phosphorylation in human platelets has not yet been clarified.

The present study investigated the mechanisms and the roles of ADP-induced HSP27 phosphorylation on human platelets. These results showed, for the first time, that the phosphorylation levels of HSP27 were correlated with platelet granule secretion but not with platelet aggregation.

Materials and methods

Reagents

ADP was purchased from Sigma–Aldrich Co. (St. Louis, MO, USA). Desferrioxamine, PD98059 and SB203580 were purchased from Calbiochem-Novabiochem Corporation (La Jolla, CA).

Preparation of platelets

To preserve steady state conditions, blood (total of 20 ml from each healthy volunteer) was drawn while the subject was in the supine position between 8:00–9:00 AM after 15 min of rest. Blood was drawn with the minimal use of a tourniquet. Sodium citrate (14 μM) was used as an anticoagulant. Platelet-rich plasma (PRP) was obtained from blood samples including sodium citrate by centrifugation at 1000g for 12 min at room temperature. Platelet-poor plasma was prepared from residual blood by centrifugation at 3000g for 5 min. All participants signed an informed consent agreement after receiving a detailed explanation and the study was approved by the Committee of Ethics in Gifu University Graduate School of Medicine.

Measurement of platelet aggregation induced by ADP

Platelet aggregation using citrated PRP was followed in an aggregometer (PA 200 apparatus, Kowa Co. Ltd., Tokyo, Japan) at 37 °C for 5 min with a stirring speed of 800 rpm. The platelets were preincubated for 1 min, and then platelet aggregation was monitored for 4 min after the addition of various doses of ADP (0.3–3 μM). The percentage of transmittance of the isolated platelets was recorded as 0%, and that of the appropriate platelet-poor plasma (blank) was recorded as 100%.

Protein preparation after ADP stimulation

The cells were pretreated with or without 2 mM of desferrioxamine for 15 min before ADP stimulation. After the stimulation with ADP for 4 min, platelet aggregation was then terminated by the addition of an ice-cold EDTA (10 mM) solution. The mixture was centrifuged at 10,000g at 4 °C for 2 min. To measure PDGF-AB and 5-HT as described below, the supernatant was isolated and stored at −20 °C for subsequent ELISA. For Western blot analysis, the pellet was washed twice with phosphate-buffered saline and then lysed and immediately boiled in a lysis buffer containing 62.5 mM Tris/Cl, pH 6.8, 2% sodium dodecyl sulfate (SDS), 50 mM dithiothreitol, and 10% glycerol as previously described [21].

Treatment with MAPK inhibitors on ADP-induced platelet aggregation

Either PD98059, a MEK1/2 inhibitor, or SB203580, a p38 MAPK inhibitor, were added to PRP and incubated at 37 °C for 5 min, then ADP-induced platelet aggregation (3 μM) was measured as described in above section.

Western blot analysis

A Western blot analysis was performed as described previously [21]. Simply, SDS–polyacrylamide gel electrophoresis (PAGE) was performed by the method of Laemmli [22] in a 12% or 10% polyacrylamide gel. Proteins were fractionated and transferred onto Immobilion-P membrane (PVDF). Membranes were blocked with 5% fat-free dry milk in Tris-buffered saline with 0.1% Tween 20 (TBS-T, 20 mM Tris, pH 7.6, 137 mM NaCl, 0.1% Tween) for 2 h before incubation with the indicated primary antibody. The antibodies used in these studies were anti-HSP27, anti-phospho HSP27 (Ser-15), anti-phospho HSP27 (Ser-78) (Stressgen Biotechnologies, Victoria, BC, Canada), anti-phospho HSP27 (Ser-82) (Biomol Research Laboratories, Plymouth Meeting, PA), p38 MAPK, phospho-p38 MAPK, p44/p42 MAPK, phospho-p44/p42 MAPK antibody (Cell Signaling, Inc. Beverly, MA), respectively. Peroxidase-labeled anti-mouse IgG (Santa Cruz Biotechnology, Inc., California, USA) or anti-rabbit IgG antibodies (KPL, Gaithersburg, MD, USA) were used as secondary antibodies. The first and second antibodies were diluted for optimum concentration respectively with 5% fat-free dry milk in TBS-T. Peroxidase activity on PVDF membranes was visualized on X-ray film by means of an ECL Western blotting detection system (GE Healthcare, Buckinghamshire, UK) as manufacturer's protocol. The densitometric analysis was performed using Molecular Analyst/Macintosh (Bio-Rad Laboratories, Hercules, CA).

Immunoprecipitation

Immunoprecipitation of the extracts of cells was carried out in 1.5 ml microcentrifuge tubes using agarose conjugated anti-actin antibody (Santa Cruz). The anti-actin antibody (20 μg IgG) were added to 1 ml TNE buffer (10 mM Tris–HCl pH

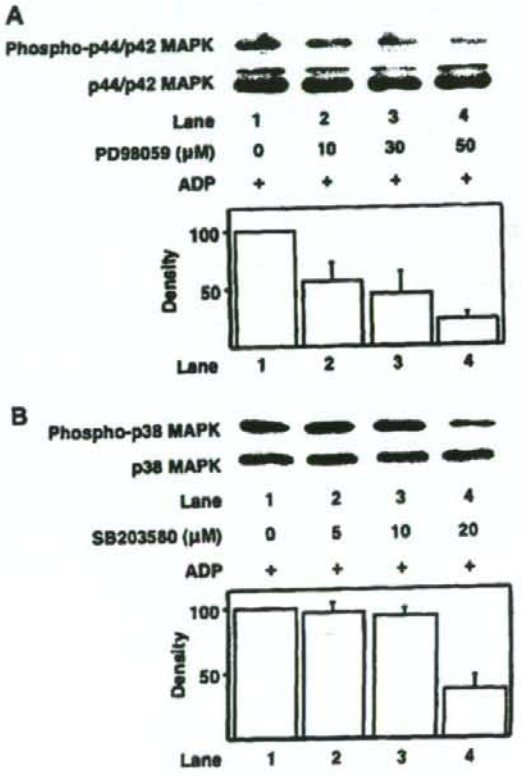

Fig. 2. Effects of PD98059 and SB203580 on the phosphorylation p44/p42 MAPK and p38 MAPK in human platelets. Various dose of (A) PD98059, a specific inhibitor of MEK1/2 or (B) SB203580, a specific inhibitor of p38 MAPK, were added to PRP and incubated at 37 °C for 5 min without stirring. PRP was followed in an aggregometer at 37 °C for 5 min with a stirring speed of 800 rpm; PRP was preincubated for 1 min with stirring, then platelet aggregation was monitored for 4 min after the addition of 3 μM of ADP. Aggregation was terminated by the addition of an ice-cold EDTA (10 mM) solution. The extracts of cells were then subjected to SDS–PAGE using antibodies against phospho-specific p44/p42 MAPK, p44/p42 MAPK, phospho-specific p38 MAPK, or p38 MAPK. Lower graph shows the quantification data of the amount of the indicated protein shown in the upper figures. Representative results from at least three independent experiments are shown.

7.8, 1% Nonidet P-40, 0.15 M NaCl, 1 mM EDTA)-solubilized platelet, and the mixture was incubated at room temperature for over-night at 4 °C. After incubation, the antigen–antibody complexes were pelleted by centrifugation and used for Western blot analysis.

Measurement of plasma PDGF-AB and 5-HT levels

The plasma PDGF-AB and 5-HT levels in samples were determined using PDGF-AB Quantikine and Serotonin ELISA purchased from R&D (Minneapolis, MN) and IBL-Hamburg (Hamburg, Germany), respectively.

Statistical analysis

The data were analyzed by Mann–Whitney's *U*-test, and a $p < 0.05$ was considered significant. All data are presented as means ± SEM.

Results

Effect of ADP on the phosphorylation of HSP27 or MAPKs in human platelets

We first examined the dose dependent effect of ADP on HSP27 phosphorylation in human platelets by a Western blot analysis. As shown in Fig. 1A, ADP induced HSP27 phosphorylation (Ser-15, Ser-78 and Ser-82) at a dose of 3 μM in human platelets. To separate the effect of ADP (as an endogenous inducer of platelets activation) from the effect of ADP as a cause of oxidative stress, we next examined the effect of desferrioxamine, which chelates iron and Cu atoms, on the ADP-induced phosphorylation of HSP27 and found that there are no significant differences between with or without desferrioxamine in the phosphorylation (Fig. 1B). We also confirmed the similar results by the ELISA on the level of PDGF-AB and 5-HT (data not shown), indicating that there are no significant effect of ADP as a cause of oxidative stress.

Since it has been reported that HSP27 phosphorylation is catalyzed by the MAPK superfamily (p38 MAPK, SAPK/JNK, and p44/p42 MAPK) [11,19,20], we next examined the effect of ADP on the activation of these MAPKs in human platelets. In results, ADP induced the phosphorylation of p44/p42 MAPK and p38 MAPK at a dose of 3 μM. But, ADP failed to induce the phosphorylation of SAPK/JNK in human platelets (Fig. 1C).

Effects of MAPK inhibitors on the ADP-induced platelet aggregation and phosphorylation of HSP27

To elucidate the roles of p44/p42 MAPK or p38 MAPK in ADP-induced platelet aggregation, we tested the effects of PD98059, a specific inhibitor of MEK1/2 [23], or SB203580, a specific inhibitor of p38 MAPK [24] on ADP-induced platelet aggregation. We first treated cells with PD98059 and SB203580 at several concentrations and confirmed that 50 μM of PD98059 and 20 μM of SB203580 clearly suppressed ADP-induced phosphorylation of p44/p42 MAPK and p38 MAPK, respectively (Fig. 2A and B, respectively). However, PD98059 had little effect on the ADP-induced platelet aggregation (Fig. 3A), even though the cells were treated with 50 μM of PD98059. Similarly, even 20 μM of SB203580 did not affect the platelet aggregation (Fig. 3B). Based on these results, it seems unlikely that p44/p42 MAPK or p38 MAPK is involved in the ADP-induced platelet aggregation.

We next examined the effects of PD98059 or SB203580 on ADP-induced phosphorylation of HSP27 in human platelets. PD98059 suppressed ADP-induced phosphorylation levels of HSP27 (Ser-15, Ser-78 and Ser-82) at doses over 10 μM (Fig. 4A). In addition, SB203580 also attenuated ADP-induced phosphorylation levels of HSP27 (Ser-15, Ser-78 and Ser-82) at doses over 5 μM (Fig. 4B). These results clearly suggest that both of p44/p42 MAPK and p38 MAPK pathway are involved in ADP-induced phosphorylation of HSP27.

Effects of MAPK inhibitors on the ADP-induced platelet granule secretion

ADP has been recognized to provoke granule secretion as well as aggregation in human platelets [25]. It has also been recognized that platelets contain various kinds of proteins, including PDGF-AB and 5-HT, in α-granules and dense granules, respectively, and thus

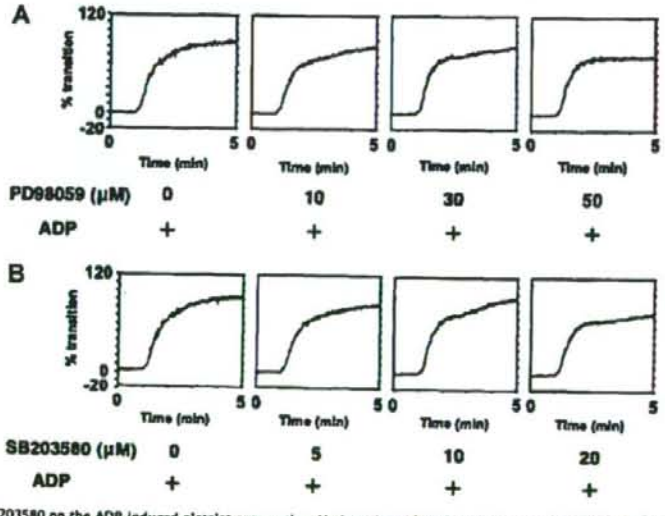

Fig. 3. Effects of PD98059 and SB203580 on the ADP-induced platelet aggregation. Various dose of (A) PD98059, a specific inhibitor of MEK1/2 or (B) SB203580, a specific inhibitor of p38 MAPK, were added to PRP and incubated at 37 °C for 5 min without stirring. PRP was followed in an aggregometer at 37 °C for 5 min with a stirring speed of 800 rpm: PRP was preincubated for 1 min with stirring, then platelet aggregation was monitored for 4 min after the addition of 3 μM of ADP. The percentage of transmittance of the isolated platelets was recorded as 0%, and that of the appropriate platelet-free plasma (blank) was recorded as 100%.

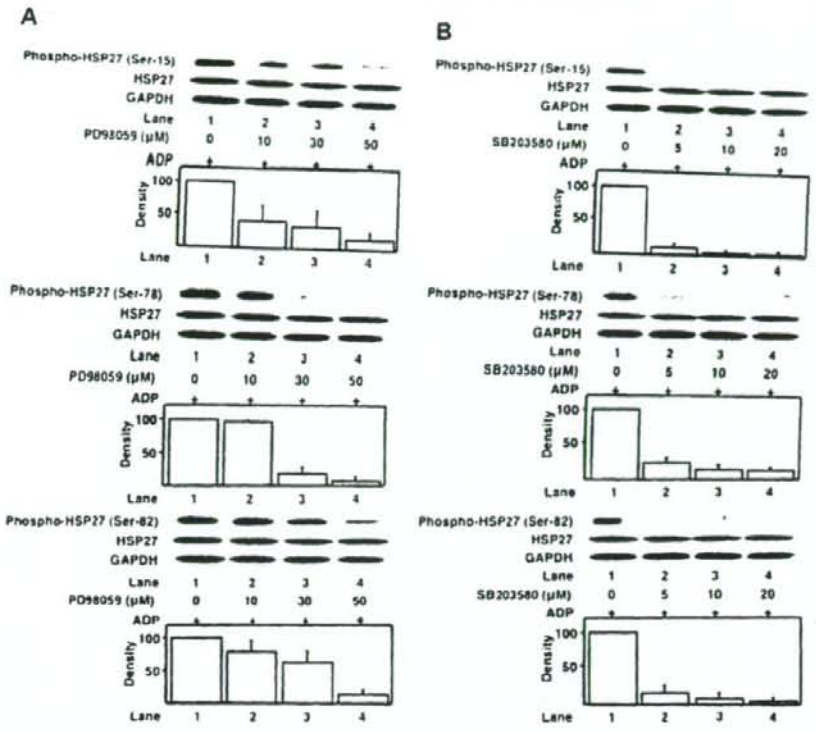

Fig. 4. Effects of PD98059 and SB203580 on the ADP-induced phosphorylation of HSP27. Various dose of (A) PD98059, a specific inhibitor of MEK1/2 or (B) SB203580, a specific inhibitor of p38 MAPK, were added to PRP and incubated at 37 °C for 5 min without stirring. PRP was followed in an aggregometer at 37 °C for 5 min with a stirring speed of 800 rpm; PRP was preincubated for 1 min with stirring, then platelet aggregation was monitored for 4 min after the addition of 3 μM of ADP. Aggregation was terminated by the addition of an ice-cold EDTA (10 mM) solution. The extracts of cells were subjected to SDS–PAGE using antibodies against total HSP27, Ser-15, Ser-78, Ser-82 phospho-specific HSP27 and GAPDH. Lower graph shows the quantification data of the amount of the indicated protein shown in the upper figures. Representative results from at least three independent experiments are shown.

secrete these proteins upon activation [1]. To evaluate whether p44/p42 MAPK or p38 MAPK play a part in granule secretion, we next examined the effect of PD98059 or SB203580 on the ADP-induced PDGF-AB or 5-HT secretion from human platelets. Both PD98059 and SB203580 significantly inhibited the ADP-induced PDGF-AB and 5-HT secretion (Fig. 5A–D). Thus, PD98059 (50 μM) caused about 95% reduction both in the ADP-induced PDGF-AB and 5-HT secretion compared to those of ADP alone. Similarly, SB203580 (20 μM) caused about 80% reduction in the ADP-induced PDGF-AB and 5-HT secretion, respectively, as compared to those of ADP alone. These results suggest that both p44/p42 MAPK and p38 MAPK play an important role in ADP-induced granule secretion in human platelets. In addition, it is probable that the inhibitory effects of ADP-induced HSP27 phosphorylation by PD98059 or SB203580 were correlated with the decrease of ADP-induced granule secretion in human platelets (Figs. 4 and 5).

Discussion

In the present study, we focused on the mechanisms and the roles of HSP27 phosphorylation in human platelets. Our results showed for the first time that decreased phosphorylation levels of HSP27 by the inhibition of p44/p42 MAPK or p38 MAPK were correlated with the suppression of platelet granule secretion but not with platelet aggregation. Furthermore, the inhibition of either the p44/p42 MAPK or p38 MAPK pathways has no effect on ADP-induced platelet aggregation, which thus coincides with previous findings by McNicol and Jackson [26]. It has been recognized that HSP27 interacts with and regulates the actin cytoskeleton [27–30] which is necessary for actin-based vesicle transport. Furthermore, phosphorylated HSP27 has been reported to be associated with the activation-dependent cytoskeleton in human platelets [18]. Conformational changes of HSP27 by phosphorylation are likely to promote an increased interaction between HSP27 and actin, or between HSP27 and other actin-associated proteins. Although we examined the effect of ADP on the interaction of the phosphorylated HSP27 and actin, and found that there are no significant differences on their binding (data not shown), it is of interest to further examine the effect of phosphorylated HSP27 on regulation of actin cytoskeleton.

Although enucleated, platelets are highly organized cells rich in different types of organelles. It is well known that platelets are reactive to various stimuli and release the materials stored in the three specific granules; dense granules, α-granules and lysosomes [1]. Different types of constituents are stored in three specific granule populations. A kinetic analysis of the release of the reaction reveals that the first granules that secrete their constituents are dense granules, followed by α-granules and lysosomes [31,32]. Moreover, the first two granule populations can release almost 100% of their store, whereas lysosome secretion is always incomplete even with high concentrations of agonists. However, the differential mechanism of granule secretion among these three